# Functional analysis and anti-virulent properties of a new depolymerase from a myovirus that infects Acinetobacter baumannii capsule K45.

Peer-reviewed author version

Oliveira, H; Costa A.R.; Ferreira, A.; Konstantinides, N.; Santos, S.B.; Boon, M.; NOBEN, Jean-Paul; Lavigne, R. & Azeredo, J. (2019) Functional analysis and anti-virulent properties of a new depolymerase from a myovirus that infects Acinetobacter baumannii capsule K45.. In: Journal of Virology, 93 (4), (ART N° e01163-18).

DOI: 10.1128/JVI.01163-18
Handle: http://hdl.handle.net/1942/27782

# Functional analysis and anti-virulent properties of a new depolymerase from a myovirus that infects *Acinetobacter baumannii* capsule K45

Hugo Oliveira[1]†, Ana Rita Costa[1]†, Alice Ferreira[1], Nico Konstantinides[1], Sílvio B. Santos[1], Maarten Boon[2], Jean-Paul Noben[3], Rob Lavigne[2]and Joana Azeredo[1]

†Equal contribution

[1] CEB – Centre of Biological Engineering, LIBRO – Laboratório de Investigação em Biofilmes Rosário Oliveira, University of Minho, 4710-057 Braga, Portugal (hugooliveira@deb.uminho.pt; anaritamc@deb.uminho.pt; nico.konstantinides@gmail.com; AliceFerreira-2@hotmail.com; silviosantos@ceb.uminho.pt, jazeredo@deb.uminho.pt)

[2] Laboratory of Gene Technology, KU Leuven, Leuven, Belgium (maarten.boon@kuleuven.be; rob.lavigne@kuleuven.be)

[3] Biomedical Research Institute and Transnational University Limburg, Hasselt University, Hasselt, Belgium (jeanpaul.noben@uhasselt.be)

[*] Corresponding author:

Joana Azeredo (jazeredo@deb.uminho.pt)

Tel. + 351 253 604 419 Fax. + 351 253 604 429

**Abstract**

*Acinetobacter baumannii* is an important pathogen causative of healthcare-associated infections and is able to rapidly develop resistance to all known antibiotics including colistin. As an alternative therapeutic agent, we have isolated a novel myovirus (vB_AbM_B9) which specifically infects and makes lysis from without in strains of the K45 and K30 capsule type, respectively. Phage B9 has a genome of 93,641 bp and encodes 167 predicted proteins, of which 29 were identified by mass spectrometry. This phage holds a capsule depolymerase (B9gp69) able to digest extracted exopolysaccharides of both K30 and K45 strains and that remains active in a wide range of pH values (5 to 9), ionic strengths (0 to 500 mM), and temperatures (20 to 80°C). B9gp69 demonstrated to be non-toxic in a cell line model of the human lung, and to make the K45 strain fully susceptible to serum killing *in vitro*. Contrary to the phage, no resistance development was observed by bacteria targeted with the B9gp69. Therefore, capsular depolymerases may represent attractive antimicrobial agents against *A. baumannii* infections.

36 **IMPORTANCE**

37 Currently, phage therapy has revived interest for controlling hard-to-treat bacterial infections.
38 *Acinetobacter baumannii* is an emerging Gram-negative pathogen able to cause a variety of
39 nosocomial infections. Additionally, this species is becoming more resistant to several classes of
40 antibiotics. Herein, we describe the isolation of a novel lytic myophage B9 and its recombinant
41 depolymerase. While the phage can be a promising alternative antibacterial agent, its success in the
42 market will ultimately depend on new regulatory frameworks and general public acceptance. We
43 therefore characterised the phage-encoded depolymerase which is a natural enzyme that can be
44 more easily managed and used. To our knowledge, the therapeutic potential of phage depolymerase
45 against *A. baumannii* is still unknown. We show for the first time that K45 capsule type is an
46 important virulence factor of *A. baumannii* and that capsule removal via the recombinant
47 depolymerase activity helps the host immune system to combat the bacterial infection.

48

## Introduction

*Acinetobacter baumannii* is one of the leading nosocomial pathogens responsible for 2-10% of all Gram-negative bacterial hospital infections worldwide (1). It is associated with several hospital-acquired infections (*e.g.* ventilator-associated pneumonia, bloodstream, urinary tract and surgical wound infections) and cases of community-acquired infections, mostly on immunocompromised individuals. Mortality rates range from 19 to 54% (1). The treatment of this bacterium is becoming increasingly problematic due to the emergence of multidrug-resistant strains. Many clinical isolates are already non-susceptible to last-resort carbapenem and colistin antibiotics. In fact, carbepenem-resistant *A. baumannii* have been recently listed by the World Health Organization (WHO) as the number one priority pathogen for the development of new antimicrobials (2, 3).

Several virulence factors have been identified in Gram-negative bacilli, among which the capsular structures (k-type) that are suggested to be involved in the evasion of microbial defences and macromolecular antibiotics (4-8). In *A. baumannii*, the existence of at least 106 capsular types may reflect the sophisticated and diverse protective mechanisms developed by this pathogen (9-11).

Bacteriophages and derived enzymes can be seen as an appealing alternative treatment against drug-resistant infections (12). In particular, depolymerases are encoded by some phages to degrade the polysaccharides present in the bacterial capsules, thereby allowing phages to reach the host receptor on the cell surface and initiate infection (13, 14). An extensive *in silico* review of phage depolymerases revealed that most of these enzymes are encoded in phage structural proteins such as tail fibers, baseplates and necks and that depolymerases can be divided into two main classes: hydrolases or lyases (13). Most phages encode only one or two depolymerase motifs in the same gene, but some can be found encoding multiple depolymerases (15). The presence of depolymerisation activity in phages is usually identified by the formation of a halo surrounding phage plaques. Previously, several *A. baumannii* phages encoding depolymerases that infect specific host capsular types (K-types) K1, K2, K3, K9, K19, K27 and K44, have been reported (16-20). However, there is only one study that characterized a recombinant depolymerase demonstrating its ability to degrade capsular polysaccharides extracted from planktonic cells or biofilms matrices (21). Moreover, comparatively to endolysins, the therapeutic potential of phage depolymerases is far less explored and still remains poorly studied in *A. baumannii*.

Our group has been studying the interaction of phage-borne depolymerases with different *Acinetobacter* species (18). In this report we have isolated and characterized a phage depolymerase targeting *A. baumannii* NIPH 201 which is assigned to the K45 capsule type (22). We have functionally analysed the primary and secondary structure of the enzyme and determined the

conditions in which it is able to degrade the host capsule. The enzyme demonstrated to have an anti-virulence effect against K45 strains in a human alveolar epithelial model, to enhance serum-mediated killing, and to be refractory to the development of resistance under selective pressure.

## Material and Methods

### Bacterial strains

A panel of 21 *A. baumannii* strains were used covering a range of 22 different bacterial capsule types (K1-K3, K9, K11, K15, K30, K33, K35, K37, K40, K43-K49, K57, K73 and K83) (**Table 1**). They mostly belong to the collections of Alexandr Nemec (NIPH and ANC strains) and of the Institut Pasteur (CIP strains) (23-31). All strains were routinely grown at 37°C in trypticase soy broth (TSB) or in trypticase soy agar (TSA, 1.5 % (w/v) agar).

### Phage isolation

Phage vB_AbM_B9 was isolated from a raw sewage wastewater treatment plant (Braga, Portugal) using an enrichment procedure as previously described (18), using K45 strain NIPH 201. Purified phage plaques were propagated in solid media, collected with SM buffer, filtered, purified with PEG 8000/NaCl and titrated following standard procedures (32).

### Transmission electron microscopy

Phage particles were centrifuged (20,000 × *g*, 1 h, 4 °C), washed and suspended in tap water. A drop of phage solution was added onto copper grids provided with carbon-coated Formvar films, stained with 2% (wt/vol) uranyl acetate (pH 4.0) and observed with a Jeol JEM 1400 transmission electron microscope (TEM).

### Phage sequencing and annotation

Phage B9 genomic DNA was extracted by phenol-chloroform as previously described (33). DNA library was constructed using the KAPA DNA Library preparation kit for Illumina and sequenced (100 bp in paired-end mode) using Illumina HiSeq platform (StabVida). Reads were demultiplexed and *de novo* assembled into a single contig with an average coverage above 100x using Geneious R9 and were manually inspected. MyRAST (34) and tRNAscan-SE (35) were used to determine the ORFs and tRNAs respectively. Encoding proteins were queried against protein sequences in BLASTP, HHpred

(36) and for homology search and structured prediction. TMHMM (37) and HMMTOP (38) servers were used to predict transmembrane domains and SignalP (39) to identify possible signal peptide cleavage sites. Comparative genomic and proteomic analysis were performed with BLASTN or OrthoVenn (40), respectively, and visualized using Easyfig (41).

**Mass spectrometry**

Virion proteins were isolated by chloroform:methanol extraction (1:1:0,75 [vol/vol/vol]) on a PEG purified phage stock (>$10^{10}$ PFU/ml). The extracted protein pellet was resuspended in loading buffer (40% Glycerol [vol/vol], 4% SDS [wt/vol], 200 mM Tris-HCl [pH 6.8], 8 mM EDTA, 0.4% Bromophenol blue [wt/vol]) and heated for 5 minutes at 95°C. The protein extract was then loaded and separated on a 12% SDS-PAGE gel. After visualization by staining the gel with Gelcode™ Blue Safe Protein Stain (Thermo Scientific), gel fragments covering the entire lane of the gel were excised and subjected to trypsin digestion according to Shevchenko et al. (42). The samples were subsequently analyzed using nano-liquid chromatography-electrospray ionization tandem mass spectrometry (nanoLC-ESI-MS/MS) and peptides were identified using SEQUEST [version 1.4.0.288] (ThermoFinnigan) and Mascot [version 2.5] (Matrix Science), based on a database containing all predicted phage proteins from a six-frame translation of the genome.

**Depolymerase cloning and expression**

The C-terminal part of the ORF69 coding for a depolymerase domain (genetic region 775 bp to 2,592 bp of the ORF69) was amplified using Kapa HiFi (Kapa Biosystems) and primers forward GGATCCAACCCTAACTTAATTGCAACAAT (with BamHI restriction site), and reverse CTCGAGTTATGTGATAGTTAATAAGTTAGCAGTTG (with XhoI restriction site). The amplified gene was cloned in a pTSL vector previously constructed with a SlyD leader protein and Tobacco etch virus (TEV) recognition site in-between the SlyD protein and the polylinker (43). *Escherichia coli* BL21 cells harbouring the recombinant plasmid expressed the protein with 1 µM of IPTG at 37 °C, overnight. Cells were pelleted and suspended in lysis buffer (50 mM Tris-HCl pH 8.0, 300 mM NaCl) and disrupted by three freeze/thaw cycles and sonication (8–10 cycles with 30 s pulse and 30 s pause). The protein was purified by immobilized metal affinity chromatography (Thermo Scientific) and incubated with a TEV protease overnight at 4 °C in a protease/protein ratio of 1/100 (v/v) to cleave the SlyD leader protein. The protein was re-purified using Nickel Magnetic Beads for His 6 Tag Protein Purification (Bimake) and dialyzed in 10 mM Hepes.

145

146 **Phage and depolymerase activity spectrum**

147 The spot-on-lawn method was used to screen the host range of activity of phage B9 and its
148 recombinant depolymerase (B9gp69) towards a panel of *A. baumannii* strains of different capsular
149 types (**Table 1**). Mid-log phase bacteria were poured in TSA soft agar overlay plates (TSB with 0.6%
150 (w/v) agar) to form lawns. After drying, 5 µL of phage ($10^8$ PFU/ml) or of purified enzyme (1 µM)
151 were spotted on the petri dishes and incubated at 37 °C overnight. The visualization of clear spots or
152 opaque zones (haloes) on the bacterial lawn determined the presence of antibacterial activity for
153 phage and B9gp69, respectively. For the phage, the relative efficiency of plating (EOP) was calculated
154 by dividing the titer of the phage (PFU/ml) obtained in each isolate by the titer determined in the
155 propagating host. EOP was recorded as high (≥ 0.5) or low (< 0.5).

156

157 **Phage one-step-growth curve**

158 One-step growth curve experiments were performed on K45 strain NIPH 201 exactly as previously
159 described (44). Briefly, mid-exponential-phase cells were adjusted to an $OD_{620\ nm}$ of 1.0 and infected
160 with phage using a multiplicity of infection (MOI) of 0.001. Phage was allowed to adsorb for 5 min at
161 37 °C and 120 rpm (ES-20/60). The mixture was then pelleted (7,000 × *g*, 5 min, 4 °C) and suspended
162 in fresh TSB. Samples were repeatedly taken every 5 or 10 min for a total period of 1 h of infection to
163 determined PFUs.

164

165 **Depolymerase degradation of extracted exopolysaccharides**

166 Exopolysaccharides (EPS) were extracted from K30 strain NIPH 190, K45 strain NIPH 201, and K3
167 strain NIPH 501, using an adapted protocol (45). Briefly, *A. baumannii* strains were grown on 20 TSA
168 plates supplemented with 0.5% glucose at 37 °C for 5 days. Cells were then harvested by scraping
169 with 2.5 mL of 0.9% (w/v) NaCl per plate. The suspension was incubated with 5% phenol and
170 agitated with a stir bar for 6 h. Afterwards, cells were pelleted (10,000 x *g*, 10 min) and the
171 supernatant containing the EPS was precipitated with 5 volumes of 95% ethanol overnight at -20 °C.
172 The precipitate was spun (6,000 x *g*, 10 min), suspended in distilled deionized water and treated
173 with deoxyribonuclease I (20 µg/mL) and ribonuclease (40 µg/mL) at 37 °C for 1 h. The digestion was
174 quenched by heating at 65 °C for 10 min, and samples were lyophilized.

175 The activity of the B9gp69 on extracted EPS was determined using the 3,5-dinitrosalicylic acid (DNS)
176 test to quantify sugar reducing ends. EPS were dissolved into 20 mM of different buffer systems

(Sodium citrate pH 5-6, Hepes pH 7-8, and Boric acid pH 9) to a final concentration of 5 mg/mL, and incubated with the B9gp69 at 0.1 µM or with buffer (control) at 37 °C for 1 h. At optimal pH, the B9gp69 activity was also screened in different ionic strengths (0-500 mM NaCl concentration) and temperatures (20 °C to 80 °C) for 1 h. The reaction was stopped by heat inactivation (100 °C, 15 min) and centrifuged (8,000 x *g*, 2 min) to remove the denatured enzyme. Afterwards, 100 µL of the DNS reagent at 10 mg/mL (Sigma-Aldrich) was added to an equal volume of the digested products, heated to 100 °C for 5 min and the absorbance was measured at 535 nm. Results were expressed as relative activity in percentage.

**Circular dichroism spectroscopy**

The secondary structure and the thermostability of the B9gp69 was analysed by circular dichroism in the far-UV region, using a Jasco J-1500 CD spectrometer equipped with a water-cooled Peltier unit. The spectrum was obtained using proteins dialyzed in 10 mM potassium phosphate buffer (pH 7) to a concentration of 10 µM, from 190 to 250 nm, with 1 nm steps, scanning speed of 20 nm/min, high sensitivity and 16 s response time. Three consecutive scans were recorded from each sample and potassium phosphate buffer was used as blank for baseline correction. The secondary structures were estimated from spectra using the CDSSTR (46) and CONTINLL (47) routine of the DICHROWEB (48, 49) server run on the Set 4 set for a wavelength of 190–240 nm.

Thermal denaturation data were obtained by incrementing 1 °C/min and monitoring the change in ellipticity of the protein secondary structure at 215 nm, 218 nm or 222 nm from 25 °C to 90 °C. The melting curves were plotted as a function of temperature and fitted to the Boltzmann sigmoidal function.

**Phage adsorption onto depolymerase-treated cells**

Mid-exponential ($OD_{620}$ of 0.4) growing cells of K30 strain NIPH 190, K45 strain NIPH 201 and K3 strain NIPH 501 were incubated with an equal volume of B9gp69 (0.1 µM final concentration) or Hepes (for negative control) for 2 h at RT. After, cells were spun (8,000 x *g*, 2 min) and washed twice with TSB. Phage was added at a multiplicity of infection of 0.001 with and without the presence of extracted EPS (5 mg/ml) and incubated at 37 °C and 120 rpm for 5 min to allow adsorption to the cell surface. Samples were taken before and after centrifugation of the sample, to determine total phage titer and the titer of non-adsorbed phage, respectively. Phage adsorption was calculated by subtracting the amount of non-adsorbed phage to the total amount of phage. The effect of B9gp69

in the phage capacity to adsorb to cells was analysed in percentage. Significance was determined by a Student's t test for comparison between the treated and untreated groups.

**Cytotoxicity assays**

For toxicity and cell viability assays, the human lung carcinoma cell line A549 (ATCC CCL-185) was used. Cells were maintained in Dulbecco's Modified Eagle's Medium (DMEM, Biochrom) supplemented with 10% fetal bovine serum (FBS, Biochrom) and 1x ZellShield (Biochrom) at 37 °C in a humidified atmosphere at 5% $CO_2$ (HERAcell 150). A549 cells were sub-cultured every two days at 80% confluence in T-flasks (Starstedt). For the assays, cells were seeded into 96-well microtiter plates at $5x10^5$ cells/mL and incubated at 37 °C, 5% $CO_2$ for 24h. Cells were washed once with 10 mM PBS and exposed to (i) Hepes or (ii) B9gp69 (final concentration of 0.1 µM at final concentration). After an incubation of 24 h, the cell culture medium was removed, the cells were washed once with 10 mM Hepes, and then detached with Trypsin/EDTA (Biochrom). Bacterial concentration was determined by CFU quantification, and mammalian cells were stained with Trypan blue and counted using a Neubauer chamber (Marienfeld, Germany) and a microscope (Leica ATC 2000). Toxicity of B9gp69 was assessed by i) determining the concentration of viable mammalian cells and ii) quantifying the amount of soluble formazan produced by cellular reduction of MTS for 1.5 h measured at 490 nm, after cell contact with the depolymerase and compared to that obtained for the negative control.

**Human serum assay**

The ability of the depolymerase to enhance bacterial susceptibility to serum killing was tested as previously described (50). Host K45 strain NIPH 201 and non-host K3 strain NIPH 501 were grown to mid-exponential phase, diluted in TSB till $10^4$ CFU/mL and treated with Hepes, B9gp69 or heat-inactivated (100 °C, 30 min) B9gp69 for 1 h at 37 °C. Afterwards, we added human serum from healthy volunteers with a volume ratio of 1:3 and the culture was incubated for 1 h at 37 °C. Survival bacterial cells were determined by CFUs counts.

**Resistance development assay**

The frequency of bacterial variants emerging with resistance to phage or B9gp69 was determined by incubating phage (MOI of 10) or B9gp69 (0.1 µM end concentration) with ~$10^6$ CFUs/mL of K45 strain NIPH 201 in TSB for 16 h (37 °C, 120 rpm, ES-20/60). The cultures were plated to obtain

isolated bacterial colonies. These were sub-cultured three times in TSA plates to guarantee that the colonies were free of phage and B9gp69. Then 10 colonies were picked to test the sensitivity towards both phage and B9gp69 using the spot-on-lawn method. Challenged bacteria were considered as resistant when no inhibition halo was observed.

**Nucleotide sequence accession numbers**

The complete genome sequences of the *A. baumannii* phage vB_AbaM_B9 have been deposited in GenBank under accession number MH133207.

## Results

### Novel phage B9 infects K45 type *A. baumannii*

Our initial efforts focused on isolating a lytic phage infecting a K45 strain using the isolation enrichment procedure in which NIPH 2014 (a K45 strain) was incubated with a raw wastewater treatment samples. Phage B9 was isolated and tested against a panel of *A. baumannii* reference strains of 22 distinct capsular types (**Table 2**). As expected, phage B9 infected the K45 strain but made lysis from without in a K30 strain. This means that phage B9 does not infect K30. Instead, the phage is capable of lysing K30 by destruction of the cell wall from the outside due to adsorption of multiple phages to a single cell. In agreement, the one-step-growth curve of phage B9 shows it can only replicate inside the K45 strain, with a latent period of 35 min and burst size of 181 phages per infected cell (**Figure 1**). Morphologically, phage B9 plaques are characterized by clear and uniform plaques on the host strain with small haloes (2 mm in diameter) on 0.6 % agar plates (**Figure 2a**). TEM images show that B9 features a typical morphology of the *Myoviridae* family, with a 70-nm diameter icosahedral head and a 110×15-nm contractile tail (**Figure 2b**).

We further characterized phage B9 using high-throughput sequencing. Phage B9 has a 93,641 bp double-stranded DNA, a GC content of 33.6% and overall genetic organization composed of 167 predicted ORFs (**Figure 2c**). BlastN analysis showed an overall genome identity lower than 1% to other phages in the nr database. BlastP search predicted the function of 77 of the phage B9-encoded proteins, most of which resembling proteins of *Acinetobacter* unclassified myoviruses (**Table S1**). Based on OrthoVenn analysis, we found that phage B9 shares a maximum of 30 genes with phage YMC13/03/R2096 (98170 bp, 162 ORFs, KM672662), 25 genes with phage AM24 (97137 bp, 146 ORFs, KY000079), and less than 18 genes with all other phages.

**Analysis of phage B9 structural proteins**

To determine the protein composition the of phage B9 particle, the structural components were precipitated, separated by electrophoresis, trypsinized and the resulting peptides analysed by electrospray ionization-tandem mass spectrometry (**Figure 3**). Mass spectrometry allowed the identification of 29 proteins, of which 27 had a coverage of over 5% and more than one unique peptide. Among these proteins, 13 had predicted function (e.g. tail fiber, minor and major capsid proteins), eight had unknown function but were located in the morphogenetic phage module (**Figure 1**) and six were unique proteins without homologs (gp31, gp37, gp44, gp49, gp59-60), generally closely located at the predicted morphogenetic phage module. The protein carrying the depolymerase domain (gp69) used in this study was also identified, suggesting it is also part of the phage virion structure.

**Identification of B9gp69 as a capsular depolymerase**

The fact that phage B9 plaques are surrounded by halos on K45 strain lawns is indicative of bacterial cell decapsulation by depolymerases. We detected a pectate_lyase_3 domain (PF12708) in the C-terminus of B9gp69 (**Figure 4a**), although with low homology (E-value 4.9E-7). We further proved that this is a structural encoding-protein, that has no attributed function and shares relatively low identity only to *Acinetobacter* spp. proteins (<55% amino acid identity). To assess the activity of this protein, the C-terminal domain of B9gp69 was cloned, heterologously expressed and tested using the spot-on-lawn method against *Acinetobacter* strains. Like phage B9, the recombinant depolymerase (B9gp69) is active against the K30 and K45 strains (**Table 2**). In spot test, the enzyme is active down to a concentration of 0.01 µM on both capsular types (**Figure 4b**).

**Depolymerase functional analysis**

The B9gp69 activity was also tested towards extracted EPS from the K30 and K45 sensitive strains and one K3 non-sensitive strain. In agreement with the above spot-on-lawn results, the enzyme was only able to degrade polysaccharides from the K30 and K45 strains, but not from the K3 strain (**Figure 5**). Using EPS from the K45 strain, the enzyme activity was further characterized on different environmental conditions (pH, ionic strength and temperature) (**Figure 6**). The enzyme remains active in all pH values tested (pH 5-9), with an optimum around pH 5-7 (**Figure 6a**). Interestingly, the enzyme is not affected by the presence of salt up to 500 mM (**Figure 6b**). The enzyme was also

shown to be mesophilic, exhibiting optimal activity between temperatures of 20 °C and 60 °C (**Figure 6c**). At 70 °C and 80 °C, the enzyme displays a slight or substantial reduction to 73% and 53% of activity.

To gain further insight into the structure of the depolymerase, we resorted to CD spectroscopy to assess the secondary structure content. The CD spectrum demonstrated two negative dichroic minimums, one between 218 and 220 nm and another less pronounced at 212 nm, with a positive dichroic maximum at 193 nm, which are signature peaks of an α-sheet content (**Figure 7a**). In agreement, deconvolution analysis of the CD spectra using DichroWeb server demonstrated that B9gp69 folds 100 % as α-helices. The CD was also employed to measure the secondary structure stability by monitoring transitions as a function of temperature, which indicated that the B9gp69 unfolds at 51 °C (**Figure 7b**).

**Role of depolymerase in phage adsorption**

To clarify the role of the depolymerase in phage B9 infection, we performed adsorption experiments with phage B9 and hosts of different capsular types, with and without pre-treatments with the B9gp69 and in presence or absence of free EPS (**Figure 8**). The phage adsorbs more than 93.8% to non-treated K45 cells, whereas it only adsorbs 25.3% to depolymerase-treated K45 cell ($P<0.01$). Similarly, phage adsorbs 85.5% to K30 cells vs 17.8% to depolymerase-treated K30 cells. In both cases, additions of free EPS did not interfere with phage adsorption. For non-host K3 (insensitive to both phage and enzyme), no phage adsorption was observed to either wild-type or pre-treated strain.

**Depolymerase cytotoxicity on human epithelium**

To assess the safety of B9gp69, the cytotoxicity of the depolymerase was tested towards human epithelial cells. The epithelial cell line A549 was used, as the human respiratory tract is one of the main targets of this pathogen (52). The B9gp69 demonstrated a non-toxic effect towards the cells, as similar quantities of soluble formazan were detected in A549 cells after 24 hours exposure to the depolymerse (Figure 9) as in cells in control conditions. Additionally, the number of both treated and untreated bacterial cells colonizing A549 cells were similar, demonstrating a lack of antibacterial effect of the B9gp69 (data not shown).

**Serum sensitivity of depolymerase-treated bacteria**

The capacity of the depolymerase to enhance bacterial susceptibility to serum killing was tested on the K45 strain (**Figure 10**). When intact cells were added to serum, the bacterial load increased by 2 fold. In opposite, B9gp69pre-treated cells incubated with serum were reduced below detection limit (<10 CFU/mL). As expected, B9gp69 could not complement the serum killing activity against K3 strain. This is a clear indication of the enhancing effect of the B9gp69 on the bacterial susceptibility to human serum killing.

**Frequency of phage- and depolymerase-insensitive mutants**

As the emergence of resistance is a key factor when considering phage therapy, the K45 strain was challenged with phage or B9gp69 for 24 h and evaluated for the appearance of insensitive phenotypes (**Table 3**). While the phage- and enzyme-free cultures displayed a steep growth curve, cultures infected with the phage demonstrated an initial decrease of cell density followed by regrowth after 8-9h, consequence of the development of phage-insensitive variants. For the culture incubated with the B9gp69, no anti-bacterial effect was observed.

Ten bacterial colonies of each culture were selected to assess sensitivity towards the phage or B9gp69. As expected, all ten colonies grown free of phage and enzyme remained sensitive to both. For phage-challenged cultures, three colonies were insensitive to both phage and enzyme, and seven remained sensitive to both. Of these, three had a diminished EOP, while the B9gp69 remained active at the lowest concentration of 0.01 µM. For B9gp69-challenged cultures, all ten colonies remained sensitive to both phage and enzyme, indicating lack of resistant development. Of note, the enzyme was found to be active after overnight incubation with K45 cells using drop tests (data not shown).

**Discussion**

*A. baumannii* has become one of the priority human pathogens for the development of new antimicrobials due to its prevalence in hospital care units and increased multi-drug resistance. Capsular polysaccharides represents an important virulence factor for most clinical isolates of Gram-negative and Gram-positive species (53) and presumably also for *A. baumannii (11)*. To date, of 106 capsular types found in *A. baumannii*, only K1 from the *A. baumannii* strain AB307-0294 was recently shown to be a virulence factor (11). Furthermore, the prevalence of the 106 capsular types in clinical settings remains unknown due to the absence of implemented typing schemes (9). Studies on phage-encoded depolymerases and their use for recognizion and removal of specific capsules of *A. baumannii* are necessary to develop novel typing and treatment schemes, as it has been done for

370 pathogens like, *Klebsiella*, *E. coli* and *Pseudomonas* (15, 54-57). Here we demonstrate that the K45
371 capsular type is an important virulence factor and a protective barrier against the human immune
372 system. We also demonstrate for the first time that capsular depolymerases have anti-virulent
373 properties against *A. baumannii*.

374 Firstly, we have isolated B9 myovirus from sewage samples which was able to infect only K45 strains
375 and cause lysis from without on K30 strain. We hypothesized the narrow host range to be a
376 consequence of the phage using depolymerses to recognize specific host capsule, as recently
377 demonstrated for several *A. baumannii* podoviruses (17, 18). Aiming to characterize this capsular
378 depolymerase, we sequenced the genome of phage B9. Based on bioinformatics analysis, we
379 demonstrated that phage B9 is a novel *A. baumannii* infecting phage. It lacks relatedness at genomic
380 level (< 1%), and shares limited gene content (<31 out of 167 genes) only with *A. baumannii*
381 myoviruses YMC13/03/R2096 and AM24 which were recently proposed to form a new genus named
382 "R2096virus" (both share 117 genes) (58). Additionally, novel virion structural proteins were
383 identified by mass spectrometry. Therefore phage B9 is eligible to create a new genus within the
384 subfamily *Tevenvirinae*.

385 Through screening of phage-encoding proteins and mass spectrometry, we found that B9gp69 is a
386 structural protein with a conserved C-terminal pectate_lyase_3 domain of weak homology, a domain
387 that has been previously shown to be responsible for decapsulation of bacterial cells (18). By
388 comparison with other *Acinetobacter* phages, this protein is likely a new tail spike (18). The
389 recombinant depolymerase (B9gp69) harbouring the pectate_lyase_3 domain was active on K30 and
390 K45 strains. Looking that the K loci of the tested strains that are flanked by *fkpA* and *lldP* genes,
391 several conserved genes involved in the capsule export, repeat unit processing as well as non-
392 conserved genes responsible for nucleotide-sugar and glycosyltransferase biosynthesis are present
393 (**Figure 11**). Specially, several include genes for uncommon sugars such as pseudaminic acid (*psa*)
394 and legionaminic acid (*lag*), which are absent in K30 and K35 locus. At the structure level, we noticed
395 that glucose-1-6-N-acetyl-D-glucosamine and N-acetyl-D-glucosamine-1-4-N-Acetylgalactosamine
396 are bonds shared only by K30 and K45 and are therefore possible cutting sites of the B9gp69 (59).
397 Other depolymerases encoded by *Klebsiella pneumoniae* and *E. coli*-infecting phages were also
398 found to degrade specific capsule types matching the host range of their parental phages (60). Even
399 the few examples where phages encode multiple depolymerases for multiple capsule types the
400 phage host range matched to the sum of sensitive capsule types of the individual encoded-
401 depolymerases (15, 61).

402 After testing B9gp69 in several conditions, we demonstrated that it is highly active at various pH (5
403 to 9), ionic strengths (0 to 500 mM) and temperatures (20 to 80 °C). This impressive tolerance to

404 extreme conditions is probably related to the structural nature of phage depolymerases, which has
405 been designed during evolution to endure harsh external environments in order to maintain the
406 phage infectivity. Interestingly, although the B9gp69 remained active up to 80 °C, its secondary
407 structure unfolds at much lower temperature (51 °C). It is possible that the active centre of the
408 B9gp69 remains available at high temperatures to cleave the capsular polymers, being independent
409 of its secondary structure. We also noticed that the secondary content of B9gp69 made of α-helices
410 is different from the typical beta-sheet-rich structures observed so far on other *K. pneumonia* and *E.*
411 *coli* phage depolymerases, which melt at higher temperatures (> 65 °C) (54, 62). Another important
412 difference is that we used only the C-terminal region of the tail fiber which contains the
413 depolymerase activity, while all mentioned studies used the whole tail fiber gene.

414 We have also assessed the role of B9gp69 in phage adsorption. Phages typically use tail spikes or tail
415 fiber proteins to recognize various bacterial receptors, from cell wall components (e.g.
416 lipopolysaccharide, outer membrane proteins) to pili, flagella and capsules (61, 63, 64). It is also
417 common for phages to have a primary reversible and a secondary irreversible receptors (65-67). For
418 phage B9, our results indicate that the capsule surrounding the cells is essential for adsorption, since
419 the phage could no longer efficiently bind to B9gp69 pre-treated K45 cells. The fact that the
420 addiction of crude EPS did not compromise phage adsorption indicates a strong therapeutic
421 potential of the phage in presence of free carbohydrates. Also, because phage B9 infects K45 but
422 only makes lysis from without in K30 it is possible that these two capsules act as a primary phage
423 receptor, with a distinct secondary and more internal receptor. Similar findings were previously
424 reported for *E. coli* K1 phage, which infected only the wild type strain with an intact polysialic acid
425 capsule, but not the capsule-deprived cells (63). More recently, similar results were also reported for
426 a phage-borne depolymerase infecting *K. pneumonia* and *Acinetobacter pittii* species (18, 61).
427 Therefore, depolymerases recognize bacterial capsules as receptor for phage adsorption and are
428 essential to initiate infection.

429 To assess the citotoxicity and anti-virulence effect of the capsular B9gp69, we tested the enzyme in
430 mammalian cells and human serum models. In mammalian cells assay, the enzyme was found to be
431 non-toxic.. . In the human serum assay, we observed that the K45 strain was resistance to killing by
432 serum complement and that it could proliferate. Treatment with the B9gp69 had a strong effect on
433 the K45 strain, making it fully susceptible to serum killing. The lipopolysaccharide of *Acinetobacter*
434 strains has been previous linked to the bacterium increased resistance to the host immune system
435 (74). Here we show that specific capsule polymers have also an important role on the immune
436 system evasion. These results agree with previous studies with *K. pneumonia* where several capsular
437 types (e.g. K1, K5, K8, K30, K64 and K69) were shown to be resistant to serum killing (55, 61, 75).

Considering the anti-virulence and anti-serum resistance properties of the B9gp69, this enzyme is a potential antimicrobial for the control of *A. baumannii* infections. One of the major concerns about the development of novel antimicrobial strategies, where phage therapy is included, is the repetition of the mistakes made with antibiotics, which resulted in the fast emergence of resistance. So here we addressed this issue with both phage B9 and B9gp69. Bacteria were able to develop resistance to phage B9, but not to B9gp69, probably because the enzyme is not killing the cells and instead is only degrading the extracellular capsule. It is also possible that the relatively low concentration of enzyme we used (0.1 µM), due to expression limitations, was not enough to induce resistance. Nonetheless, this study showed the *in vitro* and *ex vivo* efficacy of a phage derived capsular depolymerase from a new phage infecting *A. baumannii* able to reduce the bacterial virulence and sensitize it to serum killing. Herein we provided further evidences that claim the therapeutic potential of phage derived depolymerases against *A. baumannii*, a major threat for human health.

**Acknowledgments**

This study was supported by the Portuguese Foundation for Science and Technology (FCT) under the scope of the strategic funding of UID/BIO/04469/2013 unit, COMPETE 2020 (POCI-01-0145-FEDER-006684) and the Project PTDC/BBB-BSS/6471/2014 (POCI-01-0145-FEDER-016678). This work was also supported by BioTecNorte operation (NORTE-01-0145-FEDER-000004) funded by the European Regional Development Fund under the scope of Norte2020 - Programa Operacional Regional do Norte. HO and ARC acknowledge FCT for grants SFRH/BPD/111653/2015 and SFRH/BPD/94648/2013, respectively. We acknowledge prof. Alexandr Nemec (National Institute of Public Health, Prague, Czech Republic) and prof. Ruth Hall (School of Life and Environmental Sciences, University of Sydney, Australia) who kindly provided the *A. baumannii* strains. Support from Hercules Foundation project R-3986 for JPN is also acknowledged. The work of RL and MB was supported by a GOA grant from KU Leuven and JPN acknowledges the support of Hercules Foundation project R-3986.

**Competing Interests**

The authors declare that they have no competing financial interests.

468 **Figure Legends**

469 **Figure 1. *Acinetobacter baumannii* phage B9 one-step-growth curve**. Phage curve was performed
470 using K45 host NIPH 201.

471 **Figure 2. Morphological and genomic analysis of phage B9.** A) Plaques of phage B9 on K45 *A.*
472 *baumannii* strain NIPH 201; B) TEM micrographs of phage B9 negatively stained with 2% uranyl
473 acetate. Scale bar indicates 100 nm; C) Genome map of phage B9 with 167 predicted proteins
474 coloured according to their predicted function. Proteins identified by liquid chromatography-
475 electrospray ionization-tandem mass spectrometry (nanoESI-MS/MS) are indicated. The hypothetical
476 protein with the predicted depolymerase domain (pectate_lyase_3) used in this study is also
477 highlighted.

478 **Figure 3. Analysis of phage B9 virion proteins.** Structural proteins were separated on a 12% SDS-
479 PAGE separation gel, alongside with a PageRulerTM prestained protein ladder. The entire lane was
480 cut into 13 slices, trypsinized and the resulting peptides analysed using liquid chromatography-
481 electrospray ionization-tandem mass spectrometry analysed. The resolved proteins are listed aside.

482 **Figure 4. *In silico* and *in vitro* analysis of the depolymerase of phage B9.** A) Bioinformatics analysis
483 using BlastP and HHpred output. The depolymerase domain identified and cloned in this study
484 corresponds to the phage genetic region 775 bp to 2,592 bp of the ORF69; B) Spot test of different
485 concentrations (in µM) of the B9gp69 on *Acinetobacter baumannii* K45 strain NIPH 210.

486 **Figure 5. Depolymerase activity towards extracted exopolysaccharides (EPS).** Purified EPS from
487 depolymerase-sensitive strains K45 NIPH 201 and K30 NIPH 190 and non-sensitive strain K3 NIPH
488 501 were incubated with Hepes (untreated) or B9gp69 (treated) for 1 h at 37°C. EPS cleavage was
489 quantified by the amount of sugar ends present using the DNS method. Significance was determined
490 by a Student's t test for comparison between the treated and the untreated groups. * Statistically
491 different ($P < 0.01$).

492 **Figure 6. Depolymerase activity at different environmental conditions.** The enzyme was incubated
493 with EPS extracted from *Acinetobacter* strains at different A) pH values (5-9, 0 mM NaCl, 37 °C), B)
494 ionic strengths (pH 6, 0-500 mM NaCl, 37 °C) and C) temperatures (pH 6, 0 mM NaCl and 37-80 °C).
495 The results are expressed as relative activity, comparing with the best activity value obtained, pH 6.0
496 mM, 37 °C. * Statistically significant ($P < 0.05$).

497 **Figure 7. Circular dichroism analysis of the depolymerase.** A) CD spectrum measured in the Far-UV
498 (190-260 nm) and B) melting curve acquired at 218 nm with the protein (4 µM) dialyzed in potassium
499 phosphate buffer at pH 7.

**Figure 8. Phage adsorption**. Phage B9 was adsorbed in K3, K30 and K40 using i) wild-type cells, ii) depolymerase-treated cells and iii) depolymerase-treated cells in the presence of free EPS (5 mg/ml). Results are expressed as residual PFU percentages in comparison with adsorption assays with untreated cells, as indicated in the x-axe. Error bars represent standard deviation for three repeated experiments. Significance was determined by a Student's t test for comparison between the treated and the untreated groups. * Statistically different ($P < 0.01$).

**Figure 9**. Cytotoxicity **effect of the depolymerase on human epithelium.** The cytotoxicity effect of the enzyme was measured by assessing the viability of human lung carcinoma cell line A549 (ATCC CCL-185) when incubated with B9gp69 for 24 h, measuring the soluble formazan produced by cellular reduction by MTS at 490 mn, after addition of the CellTiter 96 Aqueous One Solution Reagent. The results are expressed in percentage by comparing with Hepes as control (=100% cell viability). * Statistically significant ($P < 0.05$).

**Figure 10. Effect of the depolymerase of phage B9 on bacterial susceptibility to serum killing. Host** K45 and non-host K3 susceptibility to killing by human serum was evaluated by adding only bacteria or bacteria pre-treated with B9gp69. The enzyme was used at 0.1 µM. Significance was determined by Student's *t* test (*, $P < 0.001$).

**Figure 11. K locus variation of *Acinetobacter baumannii* strains**. The capsular synthesis loci were represented with EasyFig drawn at scale (left) or using a table (right). Capsular polysaccharide clusters were annotated following the Hall-Kenyon nomenclature (59, 76, 77). The K locus genes are coloured according to function. The K locus is flanked by *fkpA* and *lldP* genes marked in black. Loci is accessible by the GenBank entries listed in **Table 1**. Unk – gene with unknown function; Trsp – transposase.

**Table 1. *Acinetobacter baumannii* strains used in this study.** For all strains, the specimen, origin, sequence types (ST) according the multilocus sequence analysis, capsular type (K) and respective accession numbers are given. Sequence types refer to the Pasteur scheme. Allocation of the capsular genes and respective coordinates are provided in the GenBank accession no. column. K-type - determined capsule structure; N/A - capsule structure is not available.

**Table 2. Activity spectrum on *A. baumannii* capsular types.** Drop test of phage and recombinant depolymerase were spotted in bacterial lawns to visualise activity. For the phage, the relative efficiency of plating (EOP) was calculated as the titer of the phage (PFU/ml) for each isolate divided by the titer for the propagating host and recorded as high (≥ 0.5) or low (< 0.5). EOP was also performed to distinguish productive infection (lysis) from lysis from without phenomena by the appearance of cell lysis only in the first dilution(s) for the latter case. K-type - determined capsule structure; N/A - capsule structure is not available; LFW – lysis from without

**Table 3. Activity spectrum of depolymerase B9gp69 on *A. baumannii* isolated in this study.** K45 NIPH 201 cells were incubated with SM buffer, phage or B9gp69 and afterwards tested for their sensitivity against the phage or the B9gp69 using drop tests. For the phage, the relative efficiency of plating (EOP) was calculated as the titer of the phage (PFU/ml) for each isolate divided by the titer for the propagating host and recorded as high (≥ 0.5) or low (< 0.5). EOP was also performed to distinguish productive infection (lysis) from lysis from without phenomena by the appearance of cell lysis only in the first dilution(s) for the latter case.

## References


1. **Joly-Guillou ML**. 2005. Clinical impact and pathogenicity of *Acinetobacter*. Clin Microbiol Infect **11**:868-73.
2. **Bonnin RA, Cuzon G, Poirel L, Nordmann P**. 2013. Multidrug-resistant *Acinetobacter baumannii* clone, France. Emerg Infect Dis **19**:822-3.
3. **Qureshi ZA, Hittle LE, O'Hara JA, Rivera JI, Syed A, Shields RK, Pasculle AW, Ernst RK, Doi Y**. 2015. Colistin-resistant *Acinetobacter baumannii*: beyond carbapenem resistance. Clin Infect Dis **60**:1295-303.
4. **Spinosa MR, Progida C, Tala A, Cogli L, Alifano P, Bucci C**. 2007. The *Neisseria* meningitidis capsule is important for intracellular survival in human cells. Infect Immun **75**:3594-603.
5. **Zaragoza O, Chrisman CJ, Castelli MV, Frases S, Cuenca-Estrella M, Rodriguez-Tudela JL, Casadevall A**. 2008. Capsule enlargement in *Cryptococcus neoformans* confers resistance to oxidative stress suggesting a mechanism for intracellular survival. Cell Microbiol **10**:2043-57.
6. **Yoshida K, Matsumoto T, Tateda K, Uchida K, Tsujimoto S, Yamaguchi K**. 2000. Role of bacterial capsule in local and systemic inflammatory responses of mice during pulmonary infection with *Klebsiella pneumoniae*. J Med Microbiol **49**:1003-10.
7. **Llobet E, Tomas JM, Bengoechea JA**. 2008. Capsule polysaccharide is a bacterial decoy for antimicrobial peptides. Microbiology **154**:3877-86.
8. **Geisinger E, Isberg RR**. 2015. Antibiotic modulation of capsular exopolysaccharide and virulence in *Acinetobacter baumannii*. PLoS Pathog **11**:e1004691.
9. **Kenyon JJ, Shashkov AS, Senchenkova SN, Shneider MM, Liu B, Popova AV, Arbatsky NP, Miroshnikov KA, Wang L, Knirel YA, Hall RM**. 2017. *Acinetobacter baumannii* K11 and K83 capsular polysaccharides have the same 6-deoxy-l-talose-containing pentasaccharide K units but different linkages between the K units. Int J Biol Macromol **103**:648-655.
10. **Lees-Miller RG, Iwashkiw JA, Scott NE, Seper A, Vinogradov E, Schild S, Feldman MF**. 2013. A common pathway for O-linked protein-glycosylation and synthesis of capsule in *Acinetobacter baumannii*. Mol Microbiol **89**:816-30.
11. **Russo TA, Luke NR, Beanan JM, Olson R, Sauberan SL, MacDonald U, Schultz LW, Umland TC, Campagnari AA**. 2010. The K1 capsular polysaccharide of *Acinetobacter baumannii* strain 307-0294 is a major virulence factor. Infect Immun **78**:3993-4000.
12. **Drulis-Kawa Z, Majkowska-Skrobek G, Maciejewska B**. 2015. Bacteriophages and phage-derived proteins--application approaches. Curr Med Chem **22**:1757-73.
13. **Pires DP, Oliveira H, Melo LD, Sillankorva S, Azeredo J**. 2016. Bacteriophage-encoded depolymerases: their diversity and biotechnological applications. Appl Microbiol Biotechnol **100**:2141-51.
14. **Yan J, Mao J, Xie J**. 2014. Bacteriophage polysaccharide depolymerases and biomedical applications. BioDrugs **28**:265-74.
15. **Pan YJ, Lin TL, Chen CC, Tsai YT, Cheng YH, Chen YY, Hsieh PF, Lin YT, Wang JT**. 2017. *Klebsiella* Phage PhiK64-1 Encodes Multiple Depolymerases for Multiple Host Capsular Types. J Virol **91**.
16. **Lai MJ, Chang KC, Huang SW, Luo CH, Chiou PY, Wu CC, Lin NT**. 2016. The Tail Associated Protein of *Acinetobacter baumannii* Phage PhiAB6 Is the Host Specificity Determinant Possessing Exopolysaccharide Depolymerase Activity. Plos One **11**:e0153361.
17. **Popova AV, Lavysh DG, Klimuk EI, Edelstein MV, Bogun AG, Shneider MM, Goncharov AE, Leonov SV, Severinov KV**. 2017. Novel Fri1-like Viruses Infecting *Acinetobacter baumannii*-vB_AbaP_AS11 and vB_AbaP_AS12-Characterization, Comparative Genomic Analysis, and Host-Recognition Strategy. Viruses **9**.
18. **Oliveira H, Costa AR, Konstantinides N, Ferreira A, Akturk E, Sillankorva S, Nemec A, Shneider M, Dotsch A, Azeredo J**. 2017. Ability of phages to infect *Acinetobacter*

*calcoaceticus-Acinetobacter baumannii* complex species through acquisition of different pectate lyase depolymerase domains. Environ Microbiol doi:10.1111/1462-2920.13970.

19. **Merabishvili M, Vandenheuvel D, Kropinski AM, Mast J, De Vos D, Verbeken G, Noben JP, Lavigne R, Vaneechoutte M, Pirnay JP**. 2014. Characterization of newly isolated lytic bacteriophages active against *Acinetobacter baumannii*. Plos One **9**:e104853.
20. **Peng F, Mi Z, Huang Y, Yuan X, Niu W, Wang Y, Hua Y, Fan H, Bai C, Tong Y**. 2014. Characterization, sequencing and comparative genomic analysis of vB_AbaM-IME-AB2, a novel lytic bacteriophage that infects multidrug-resistant *Acinetobacter baumannii* clinical isolates. BMC Microbiol **14**:181.
21. **Hernandez-Morales AC, Lessor LL, Wood TL, Migl D, Mijalis EM, Russell WK, Young RF, Gill JJ**. 2018. Genomic and Biochemical Characterization of *Acinetobacter* Podophage Petty Reveals a Novel Lysis Mechanism and Tail-Associated Depolymerase Activity. J Virol doi:10.1128/JVI.01064-17.
22. **Shashkov AS, Kenyon JJ, Arbatsky NP, Shneider MM, Popova AV, Miroshnikov KA, Volozhantsev NV, Knirel YA**. 2015. Structures of three different neutral polysaccharides of *Acinetobacter baumannii*, NIPH190, NIPH201, and NIPH615, assigned to K30, K45, and K48 capsule types, respectively, based on capsule biosynthesis gene clusters. Carbohydr Res **417**:81-88.
23. **Nemec A, Krizova L, Maixnerova M, van der Reijden TJ, Deschaght P, Passet V, Vaneechoutte M, Brisse S, Dijkshoorn L**. 2011. Genotypic and phenotypic characterization of the *Acinetobacter calcoaceticus-Acinetobacter baumannii* complex with the proposal of *Acinetobacter pittii* sp. nov. (formerly *Acinetobacter* genomic species 3) and *Acinetobacter nosocomialis* sp. nov. (formerly *Acinetobacter* genomic species 13TU). Res Microbiol **162**:393-404.
24. **Touchon M, Cury J, Yoon EJ, Krizova L, Cerqueira GC, Murphy C, Feldgarden M, Wortman J, Clermont D, Lambert T, Grillot-Courvalin C, Nemec A, Courvalin P, Rocha EP**. 2014. The genomic diversification of the whole *Acinetobacter* genus: origins, mechanisms, and consequences. Genome Biol Evol **6**:2866-82.
25. **Nemec A, Krizova L, Maixnerova M, Sedo O, Brisse S, Higgins PG**. 2015. Acinetobacter seifertii sp. nov., a member of the *Acinetobacter calcoaceticus-Acinetobacter baumannii* complex isolated from human clinical specimens. Int J Syst Evol Microbiol **65**:934-42.
26. **Hamidian M, Hall RM**. 2014. Tn6168, a transposon carrying an ISAba1-activated ampC gene and conferring cephalosporin resistance in *Acinetobacter baumannii*. J Antimicrob Chemother **69**:77-80.
27. **Hamidian M, Kenyon JJ, Holt KE, Pickard D, Hall RM**. 2014. A conjugative plasmid carrying the carbapenem resistance gene blaOXA-23 in AbaR4 in an extensively resistant GC1 *Acinetobacter baumannii* isolate. J Antimicrob Chemother **69**:2625-8.
28. **Kenyon JJ, Shneider MM, Senchenkova SN, Shashkov AS, Siniagina MN, Malanin SY, Popova AV, Miroshnikov KA, Hall RM, Knirel YA**. 2016. K19 capsular polysaccharide of *Acinetobacter baumannii* is produced via a Wzy polymerase encoded in a small genomic island rather than the KL19 capsule gene cluster. Microbiology-Sgm **162**:1479-1489.
29. **Shashkov AS, Liu B, Kenyon JJ, Popova AV, Shneider MM, Senchenkova SN, Arbatsky NP, Miroshnikov KA, Wang L, Knirel YA**. 2017. Structures of the K35 and K15 capsular polysaccharides of *Acinetobacter baumannii* LUH5535 and LUH5554 containing amino and diamino uronic acids. Carbohydrate Research **448**:28-34.
30. **Kenyon JJ, Kasimova AA, Shashkov AS, Hall RM, Knirel YA**. 2018. *Acinetobacter baumannii* isolate BAL_212 from Vietnam produces the K57 capsular polysaccharide containing a rarely occurring amino sugar N-acetylviosamine. Microbiology-Sgm **164**:217-220.
31. **Kenyon JJ, Notaro A, Hsu LY, De Castro C, Hall RM**. 2017. 5,7-Di-N-acetyl-8-epiacinetaminic acid: A new non-2-ulosonic acid found in the K73 capsule produced by an *Acinetobacter baumannii* isolate from Singapore. Scientific Reports **7**.

32. **Sambrook JaR, D.** 2001. Molecular cloning: a laboratory manual. Cold Spring Harbor, NY.
33. **Sambrook J, Russel D**. 2001. Molecular cloning: a laboratory manual. Cold Spring Harbor Labroratory Press, Cold Spring Harbor, NY.
34. **Aziz RK, Bartels D, Best AA, DeJongh M, Disz T, Edwards RA, Formsma K, Gerdes S, Glass EM, Kubal M, Meyer F, Olsen GJ, Olson R, Osterman AL, Overbeek RA, McNeil LK, Paarmann D, Paczian T, Parrello B, Pusch GD, Reich C, Stevens R, Vassieva O, Vonstein V, Wilke A, Zagnitko O**. 2008. The RAST server: Rapid annotations using subsystems technology. Bmc Genomics **9**.
35. **Lowe TM, Eddy SR**. 1997. tRNAscan-SE: A program for improved detection of transfer RNA genes in genomic sequence. Nucleic Acids Res **25**:955-964.
36. **Soding J, Biegert A, Lupas AN**. 2005. The HHpred interactive server for protein homology detection and structure prediction. Nucleic Acids Res **33**:W244-8.
37. **Kall L, Sonnhammer EL**. 2002. Reliability of transmembrane predictions in whole-genome data. FEBS Lett **532**:415-8.
38. **Tusnady GE, Simon I**. 2001. The HMMTOP transmembrane topology prediction server. Bioinformatics **17**:849-50.
39. **Bendtsen JD, Nielsen H, von Heijne G, Brunak S**. 2004. Improved prediction of signal peptides: SignalP 3.0. J Mol Biol **340**:783-95.
40. **Wang Y, Coleman-Derr D, Chen G, Gu YQ**. 2015. OrthoVenn: a web server for genome wide comparison and annotation of orthologous clusters across multiple species. Nucleic Acids Res **43**:W78-84.
41. **Sullivan MJ, Petty NK, Beatson SA**. 2011. Easyfig: a genome comparison visualizer. Bioinformatics **27**:1009-10.
42. **Shevchenko A, Wilm M, Vorm O, Mann M**. 1996. Mass spectrometric sequencing of proteins silver-stained polyacrylamide gels. Anal Chem **68**:850-8.
43. **Taylor NMI, Prokhorov NS, Guerrero-Ferreira RC, Shneider MM, Browning C, Goldie KN, Stahlberg H, Leiman PG**. 2016. Structure of the T4 baseplate and its function in triggering sheath contraction. Nature **533**:346-+.
44. **Oliveira H, Pinto G, Oliveira A, Oliveira C, Faustino MA, Briers Y, Domingues L, Azeredo J**. 2016. Characterization and genome sequencing of a *Citrobacter freundii* phage CfP1 harboring a lysin active against multidrug-resistant isolates. Appl Microbiol Biotechnol **100**:10543-10553.
45. **Lee IM, Tu IF, Yang FL, Ko TP, Liao JH, Lin NT, Wu CY, Ren CT, Wang AHJ, Chang CM, Huang KF, Wu SH**. 2017. Structural basis for fragmenting the exopolysaccharide of *Acinetobacter baumannii* by bacteriophage Phi AB6 tailspike protein. Scientific Reports **7**.
46. **Compton LA, Johnson WC**. 1986. Analysis of Protein Circular-Dichroism Spectra for Secondary Structure Using a Simple Matrix Multiplication. Analytical Biochemistry **155**:155-167.
47. **Vanstokkum IHM, Spoelder HJW, Bloemendal M, Vangrondelle R, Groen FCA**. 1990. Estimation of Protein Secondary Structure and Error Analysis from Circular-Dichroism Spectra. Analytical Biochemistry **191**:110-118.
48. **Whitmore L, Wallace BA**. 2004. DICHROWEB, an online server for protein secondary structure analyses from circular dichroism spectroscopic data. Nucleic Acids Res **32**:W668-W673.
49. **Whitmore L, Wallace BA**. 2008. Protein secondary structure analyses from circular dichroism spectroscopy: methods and reference databases. Biopolymers **89**:392-400.
50. **Fang CT, Chuang YP, Shun CT, Chang SC, Wang JT**. 2004. A novel virulence gene in *Klebsiella pneumoniae* strains causing primary liver abscess and septic metastatic complications. Journal of Experimental Medicine **199**:697-705.
51. **Moxon ER, Kroll JS**. 1990. The Role of Bacterial Polysaccharide Capsules as Virulence Factors. Current Topics in Microbiology and Immunology **150**:65-85.

52. **Peleg AY, Seifert H, Paterson DL**. 2008. *Acinetobacter baumannii*: emergence of a successful pathogen. Clinical Microbiology Reviews **21**:538-82.
53. **I.S. TCMR**. 2005. Capsular Polysaccharides and Their Role in Virulence. *In* H. RWH (ed), Concepts in Bacterial Virulence doi:10.1159/isbn.978-3-318-01116-6. Karger Publishers Basel.
54. **Majkowska-Skrobek G, Latka A, Berisio R, Maciejewska B, Squeglia F, Romano M, Lavigne R, Struve C, Drulis-Kawa Z**. 2016. Capsule-Targeting Depolymerase, Derived from *Klebsiella* KP36 Phage, as a Tool for the Development of Anti-Virulent Strategy. Viruses **8**.
55. **Pan YJ, Lin TL, Lin YT, Su PA, Chen CT, Hsieh PF, Hsu CR, Chen CC, Hsieh YC, Wang JT**. 2015. Identification of capsular types in carbapenem-resistant *Klebsiella pneumoniae* strains by wzc sequencing and implications for capsule depolymerase treatment. Antimicrob Agents Chemother **59**:1038-47.
56. **Olszak T, Shneider MM, Latka A, Maciejewska B, Browning C, Sycheva LV, Cornelissen A, Danis-Wlodarczyk K, Senchenkova SN, Shashkov AS, Gula G, Arabski M, Wasik S, Miroshnikov KA, Lavigne R, Leiman PG, Knirel YA, Drulis-Kawa Z**. 2017. The O-specific polysaccharide lyase from the phage LKA1 tailspike reduces *Pseudomonas* virulence. Sci Rep **7**:16302.
57. **Lin H, Paff ML, Molineux IJ, Bull JJ**. 2017. Therapeutic Application of Phage Capsule Depolymerases against K1, K5, and K30 Capsulated *E. coli* in Mice. Front Microbiol **8**:2257.
58. **Turner D, Ackermann HW, Kropinski AM, Lavigne R, Sutton JM, Reynolds DM**. 2017. Comparative Analysis of 37 *Acinetobacter* Bacteriophages. Viruses **10**.
59. **Shashkov AS, Kenyon JJ, Arbatsky NP, Shneider MM, Popova AV, Miroshnikov KA, Volozhantsev NV, Knirel YA**. 2015. Structures of three different neutral polysaccharides of *Acinetobacter baumannii*, NIPH190, NIPH201, and NIPH615, assigned to K30, K45, and K48 capsule types, respectively, based on capsule biosynthesis gene clusters. Carbohydr Res **417**:81-8.
60. **Majkowska-Skrobek G, Latka A, Berisio R, Maciejewska B, Squeglia F, Romano M, Lavigne R, Struve C, Drulis-Kawa Z**. 2016. Capsule-Targeting Depolymerase, Derived from *Klebsiella* KP36 Phage, as a Tool for the Development of Anti-Virulent Strategy. Viruses-Basel **8**.
61. **Hsieh PF, Lin HH, Lin TL, Chen YY, Wang JT**. 2017. Two T7-like Bacteriophages, K5-2 and K5-4, Each Encodes Two Capsule Depolymerases: Isolation and Functional Characterization. Sci Rep **7**:4624.
62. **Guo Z, Huang J, Yan G, Lei L, Wang S, Yu L, Zhou L, Gao A, Feng X, Han W, Gu J, Yang J**. 2017. Identification and Characterization of Dpo42, a Novel Depolymerase Derived from the Escherichia coli Phage vB_EcoM_ECOO78. Front Microbiol **8**:1460.
63. **Scholl D, Rogers S, Adhya S, Merril CR**. 2001. Bacteriophage K1-5 encodes two different tail fiber proteins, allowing it to infect and replicate on both K1 and K5 strains of *Escherichia coli*. J Virol **75**:2509-15.
64. **Cornelissen A, Ceyssens PJ, Krylov VN, Noben JP, Volckaert G, Lavigne R**. 2012. Identification of EPS-degrading activity within the tail spikes of the novel *Pseudomonas putida* phage AF. Virology **434**:251-6.
65. **Marti R, Zurfluh K, Hagens S, Pianezzi J, Klumpp J, Loessner MJ**. 2013. Long tail fibres of the novel broad-host-range T-even bacteriophage S16 specifically recognize *Salmonella* OmpC. Mol Microbiol **87**:818-34.
66. **Parent KN, Erb ML, Cardone G, Nguyen K, Gilcrease EB, Porcek NB, Pogliano J, Baker TS, Casjens SR**. 2014. OmpA and OmpC are critical host factors for bacteriophage Sf6 entry in Shigella. Mol Microbiol **92**:47-60.
67. **Golomidova AK, Kulikov EE, Prokhorov NS, Guerrero-Ferreira Rcapital Es C, Knirel YA, Kostryukova ES, Tarasyan KK, Letarov AV**. 2016. Branched Lateral Tail Fiber Organization in T5-Like Bacteriophages DT57C and DT571/2 is Revealed by Genetic and Functional Analysis. Viruses **8**.

68. **Hood MI, Becker KW, Roux CM, Dunman PM, Skaar EP**. 2013. genetic determinants of intrinsic colistin tolerance in *Acinetobacter baumannii*. Infect Immun **81**:542-51.

69. **Lin L, Tan B, Pantapalangkoor P, Ho T, Baquir B, Tomaras A, Montgomery JI, Reilly U, Barbacci EG, Hujer K, Bonomo RA, Fernandez L, Hancock RE, Adams MD, French SW, Buslon VS, Spellberg B**. 2012. Inhibition of LpxC protects mice from resistant *Acinetobacter baumannii* by modulating inflammation and enhancing phagocytosis. MBio **3**.

70. **Lee CR, Lee JH, Park M, Park KS, Bae IK, Kim YB, Cha CJ, Jeong BC, Lee SH**. 2017. Biology of *Acinetobacter baumannii*: Pathogenesis, Antibiotic Resistance Mechanisms, and Prospective Treatment Options. Front Cell Infect Microbiol **7**:55.

71. **Smith SGJ, Mahon V, Lambert MA, Fagan RP**. 2007. A molecular Swiss army knife: OmpA structure, function and expression. Fems Microbiology Letters **273**:1-11.

72. **Gaddy JA, Tomaras AP, Actis LA**. 2009. The *Acinetobacter baumannii* 19606 OmpA Protein Plays a Role in Biofilm Formation on Abiotic Surfaces and in the Interaction of This Pathogen with Eukaryotic Cells. Infect Immun **77**:3150-3160.

73. **Jacobs AC, Hood I, Boyd KL, Olson PD, Morrison JM, Carson S, Sayood K, Iwen PC, Skaar EP, Dunman PM**. 2010. Inactivation of Phospholipase D Diminishes *Acinetobacter baumannii* Pathogenesis. Infect Immun **78**:1952-1962.

74. **Panilaitis B, Johri A, Blank W, Kaplan D, Fuhrman J**. 2002. Adjuvant activity of emulsan, a secreted lipopolysaccharide from *Acinetobacter calcoaceticus*. Clin Diagn Lab Immunol **9**:1240-7.

75. **Lin TL, Hsieh PF, Huang YT, Lee WC, Tsai YT, Su PA, Pan YJ, Hsu CR, Wu MC, Wang JT**. 2014. Isolation of a bacteriophage and its depolymerase specific for K1 capsule of *Klebsiella pneumoniae*: implication in typing and treatment. J Infect Dis **210**:1734-44.

76. **Kenyon JJ, Hall RM**. 2013. Variation in the complex carbohydrate biosynthesis loci of *Acinetobacter baumannii* genomes. Plos One **8**:e62160.

77. **Arbatsky NP, Shneider MM, Kenyon JJ, Shashkov AS, Popova AV, Miroshnikov KA, Volozhantsev NV, Knirel YA**. 2015. Structure of the neutral capsular polysaccharide of *Acinetobacter baumannii* NIPH146 that carries the KL37 capsule gene cluster. Carbohydr Res **413**:12-5.

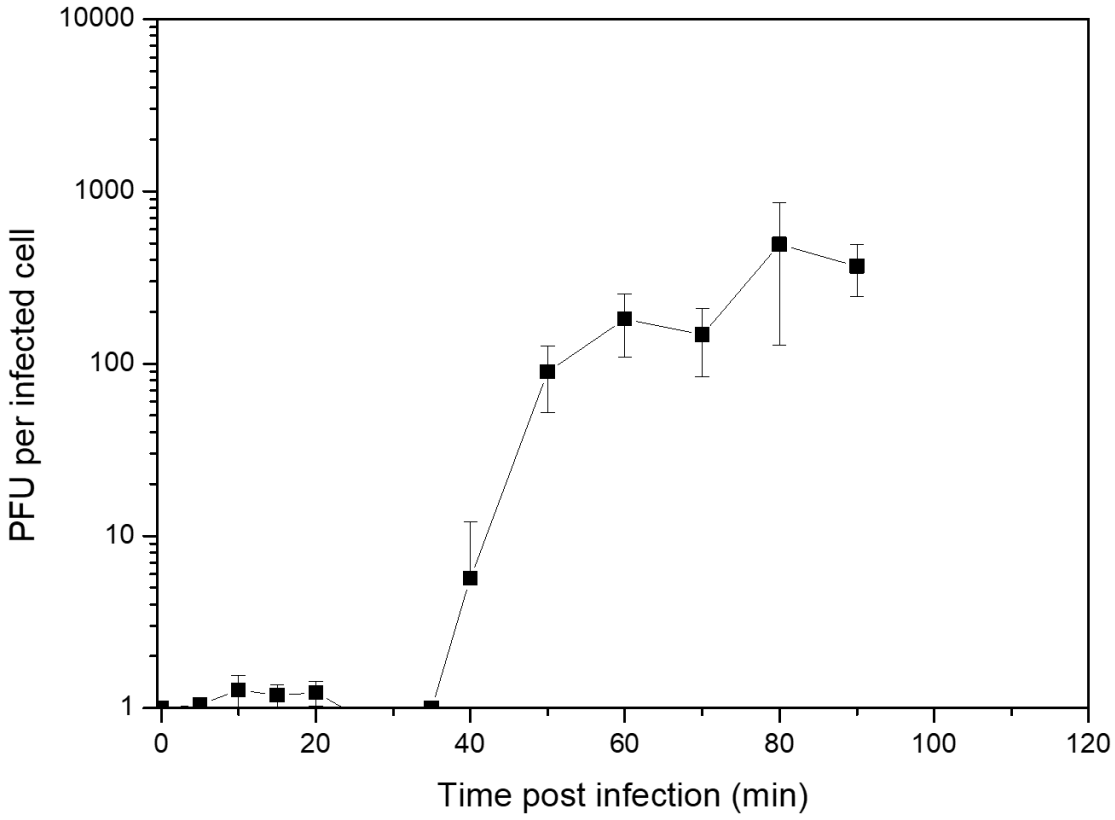

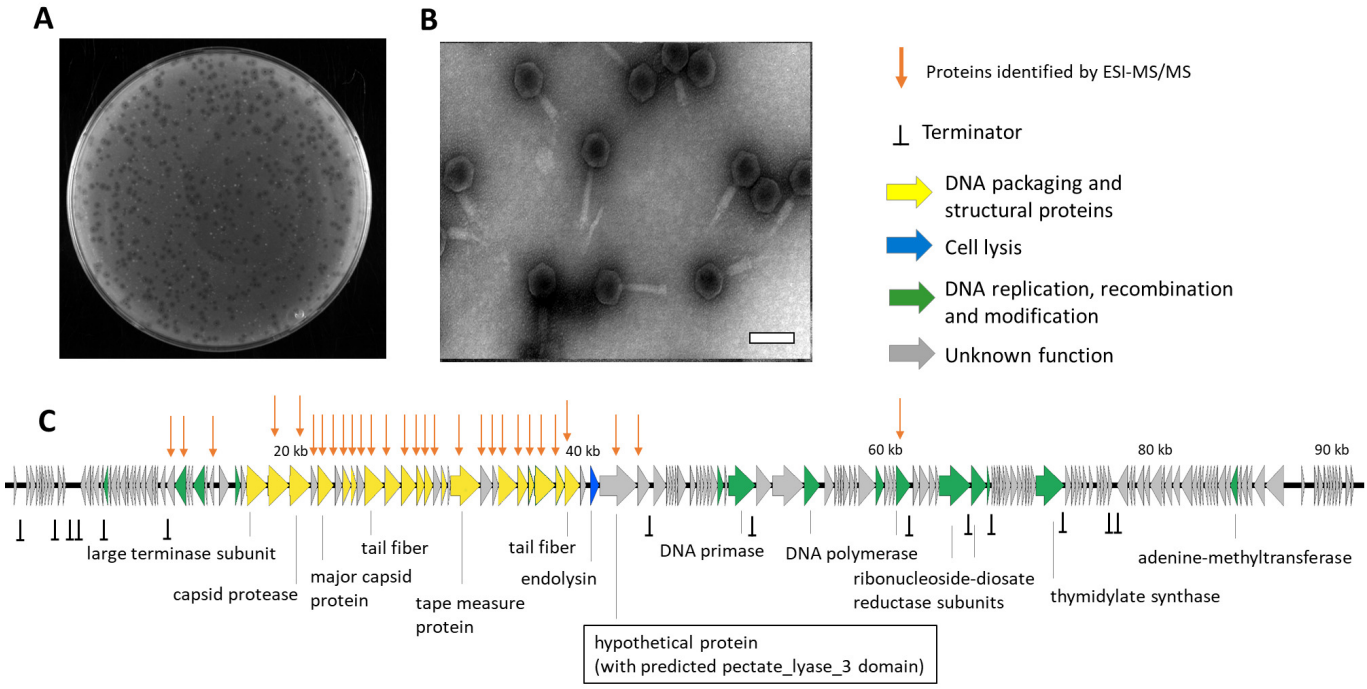

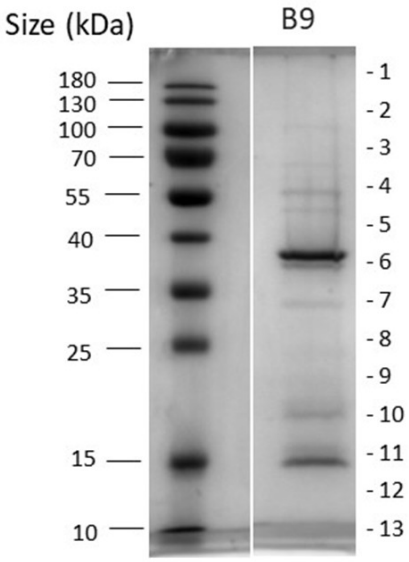


| Protein | Putative function | Band Nº (most abundant) | Protein MW (kDa) | Nº of unique peptides | Sequence coverage (%) |
|---|---|---|---|---|---|
| **gp31** | - | 10 | 20.91 | 2 | 17.10 |
| **gp32** | ClpP subunit | 8 | 29.47 | 1 | 2.72 |
| **gp37** | - | 11,12 (11) | 11.04 | 1 | 15.00 |
| **gp42** | portal protein | 2,3,4,5,7,8 (4) | 54.51 | 20 | 49.63 |
| **gp43** | capsid protease | 7,8 (8) | 53.56 | 7 | 15.60 |
| **gp44** | - | 2,4,6,7,8,9,10,11,12,13 (11) | 16.79 | 9 | 69.20 |
| **gp45** | major capsid protein | 1,2,3,4,5,6,7,8,9,10,11,12 (6) | 39.29 | 18 | 63.45 |
| **gp46** | hypothetical protein | 6,8,9,10 (10) | 19.10 | 8 | 52.80 |
| **gp47** | tail completion protein gpS | 8,9 (8) | 23.50 | 2 | 8.54 |
| **gp48** | tail tube completion protein | 11 | 15.25 | 1 | 15.70 |
| **gp49** | - | 7,8,9,10 (10) | 19.67 | 5 | 29.70 |
| **gp50** | tail fiber | 1,2,3,4,5 (4) | 47.23 | 16 | 63.47 |
| **gp51** | tail sheath protein | 2,3,4,5 (5) | 44.11 | 2 | 6.30 |
| **gp52** | tail sheath protein | 1,2,3,4,5,6,7,8,13 (4) | 37.97 | 15 | 67.45 |
| **gp53** | structural protein | 1,2,3,4,5,6,7,8,9,10,11,12 (10) | 19.51 | 5 | 36.50 |
| **gp54** | tail tube protein | 9,10 (9) | 21.35 | 6 | 36.65 |
| **gp55** | hypothetical protein | 10 | 19.82 | 6 | 45.30 |
| **gp58** | tape measure protein | 1,2,3,6,7 (3) | 74.80 | 28 | 49.02 |
| **gp59** | - | 1,2,3,4,5,6,7 (6) | 31.37 | 9 | 35.60 |
| **gp60** | - | 12 | 15.78 | 1 | 6.15 |
| **gp61** | baseplate protein gpD | 1,2,3,4 (4) | 49.72 | 10 | 26.98 |
| **gp62** | baseplate central spike protein | 2,8 (8) | 26.13 | 4 | 20.03 |
| **gp63** | baseplate wedge protein gp25 | 11 | 15.98 | 4 | 34.10 |
| **gp64** | baseplate wedge protein gpJ | 1,2,3,4,5,6,7 (4) | 52.00 | 13 | 46.70 |
| **gp65** | baseplate wedge protein gpI | 8,9 (8) | 23.51 | 6 | 26.10 |
| **gp66** | tail fiber | 2,3,4,5,6,7 (6) | 38.43 | 19 | 76.90 |
| **gp69** | hypothetical protein | 1,2,3 (2) | 94.46 | 22 | 36.25 |
| **gp70** | hypothetical protein | 1,2,3,4,5,6 (6) | 31.07 | 5 | 25.40 |
| **gp101** | DNA polymerase II | 6,7 (7) | 38.00 | 1 | 3.04 |

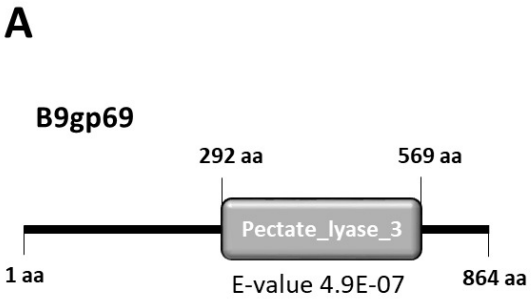


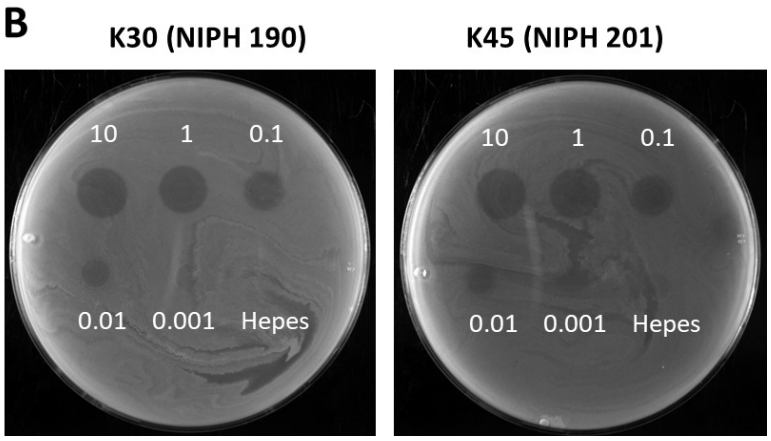

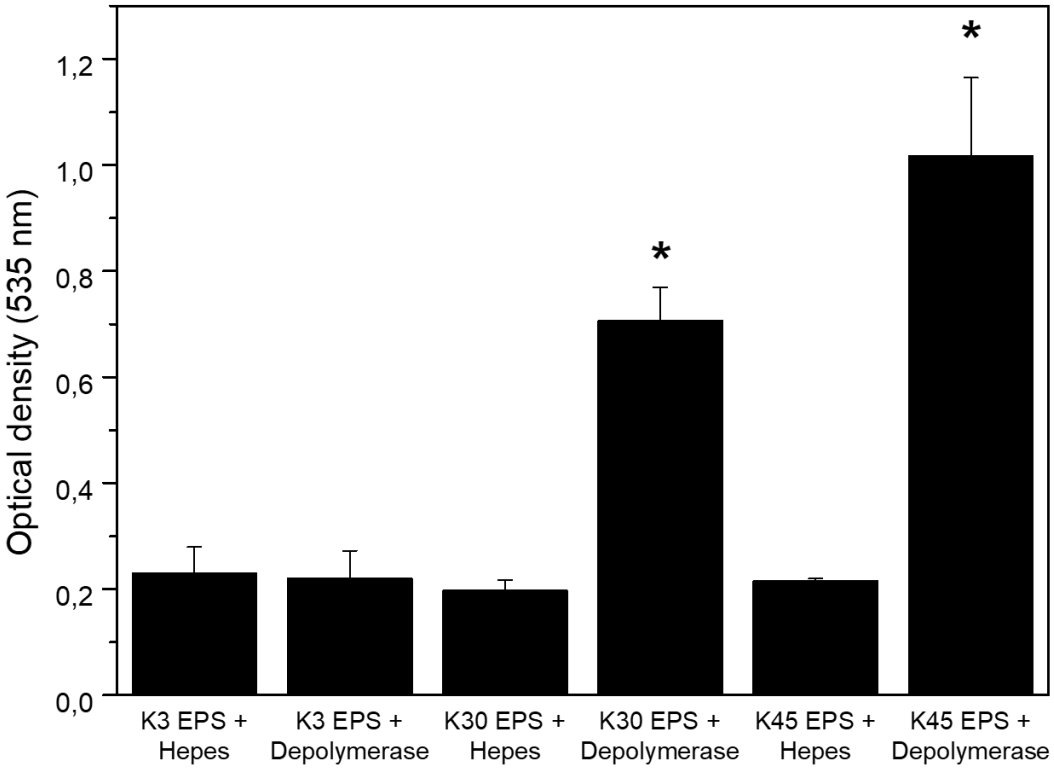

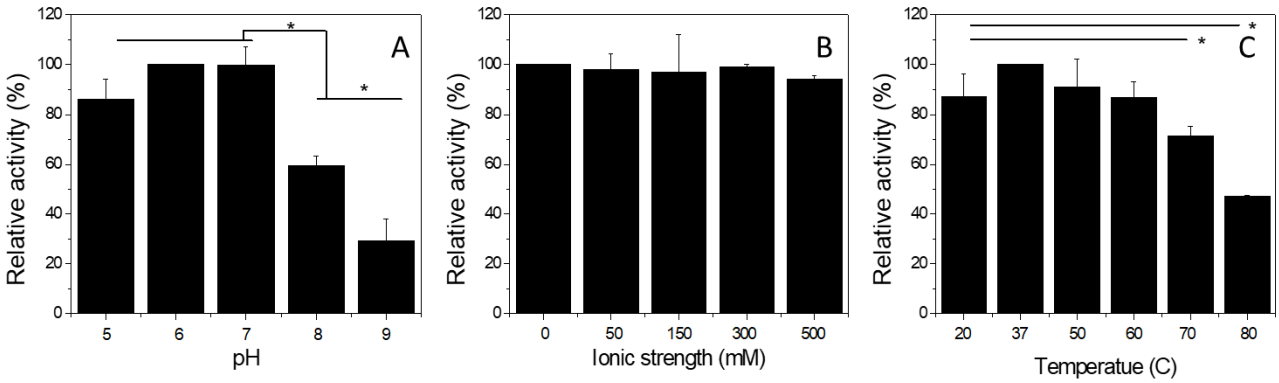

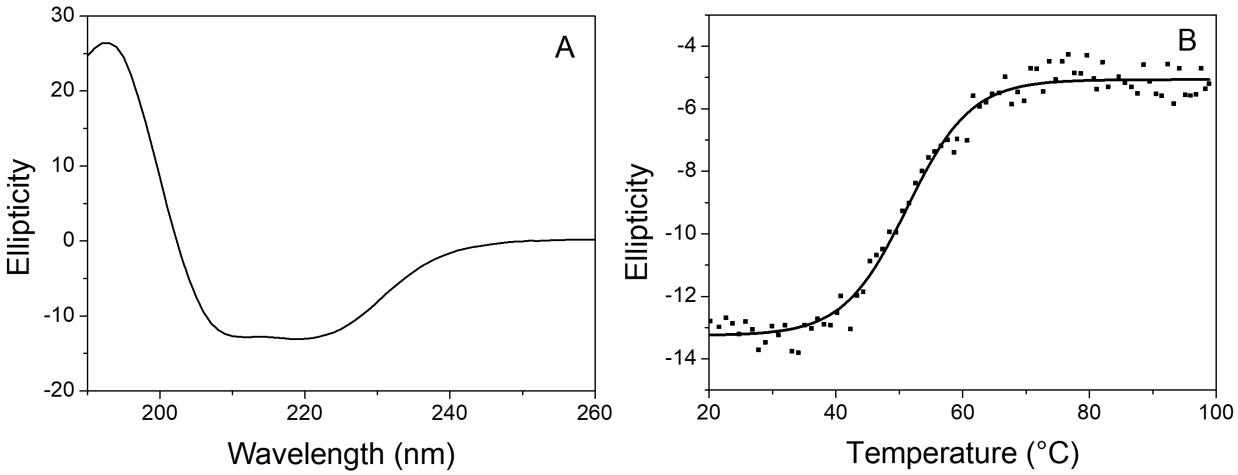

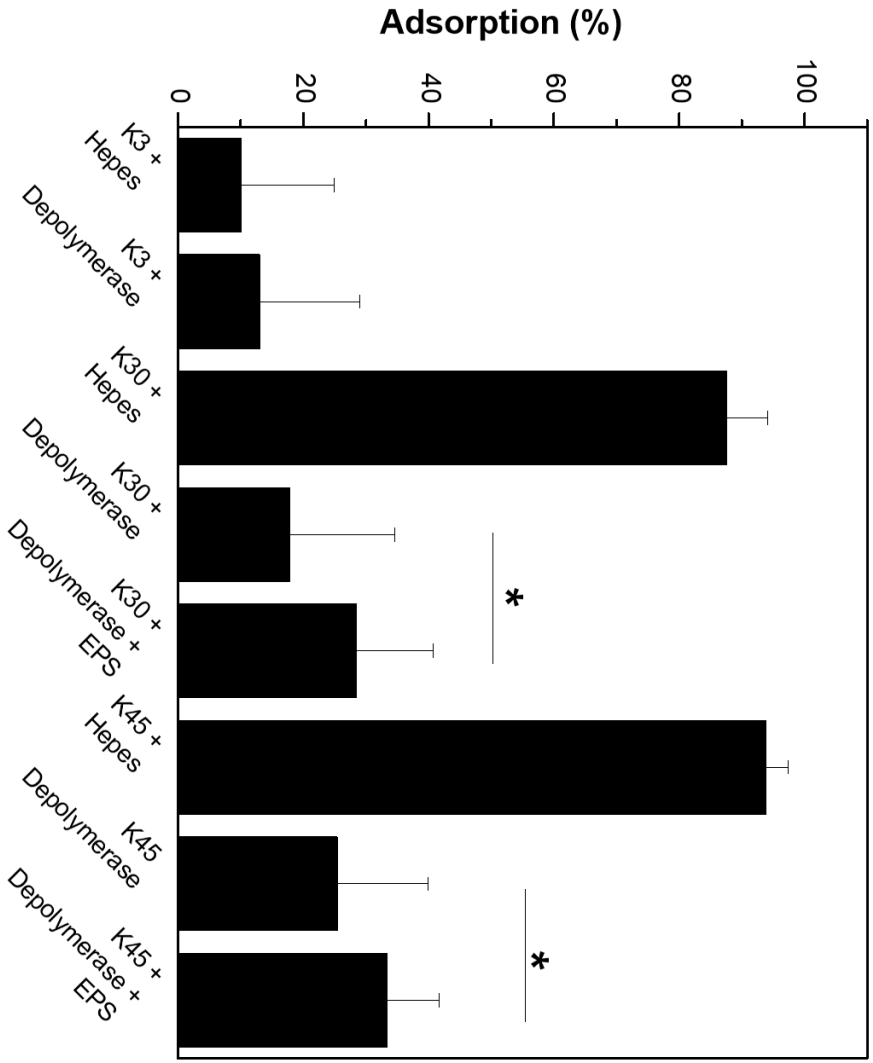

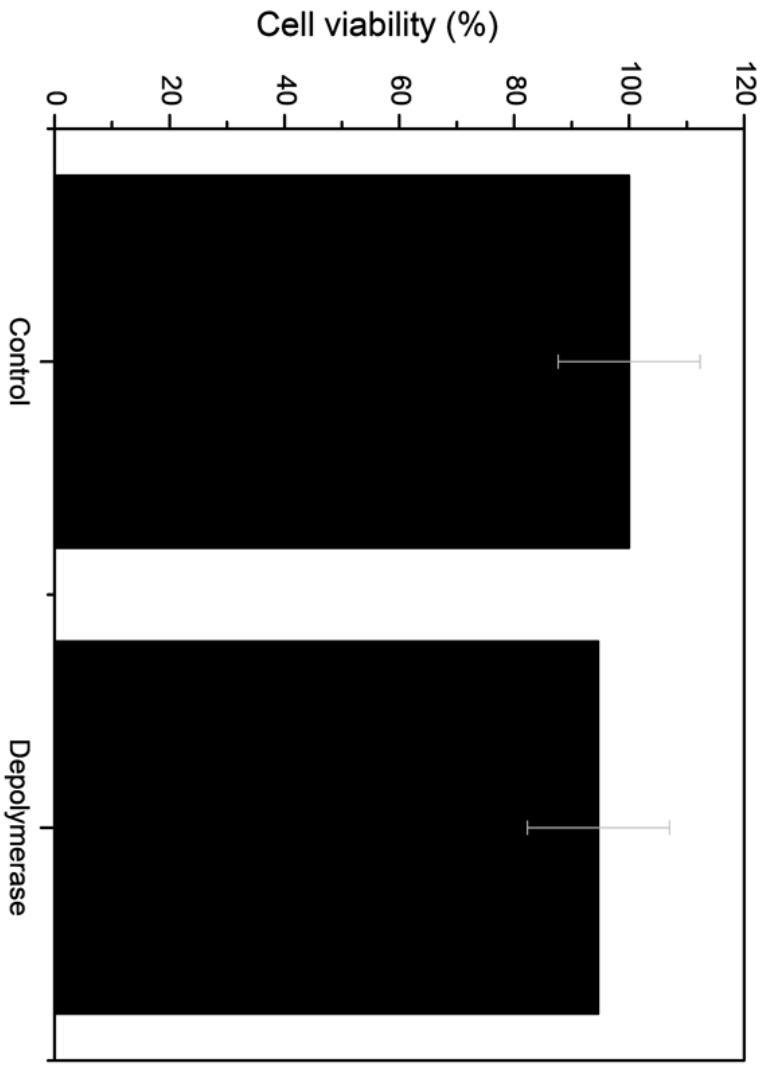

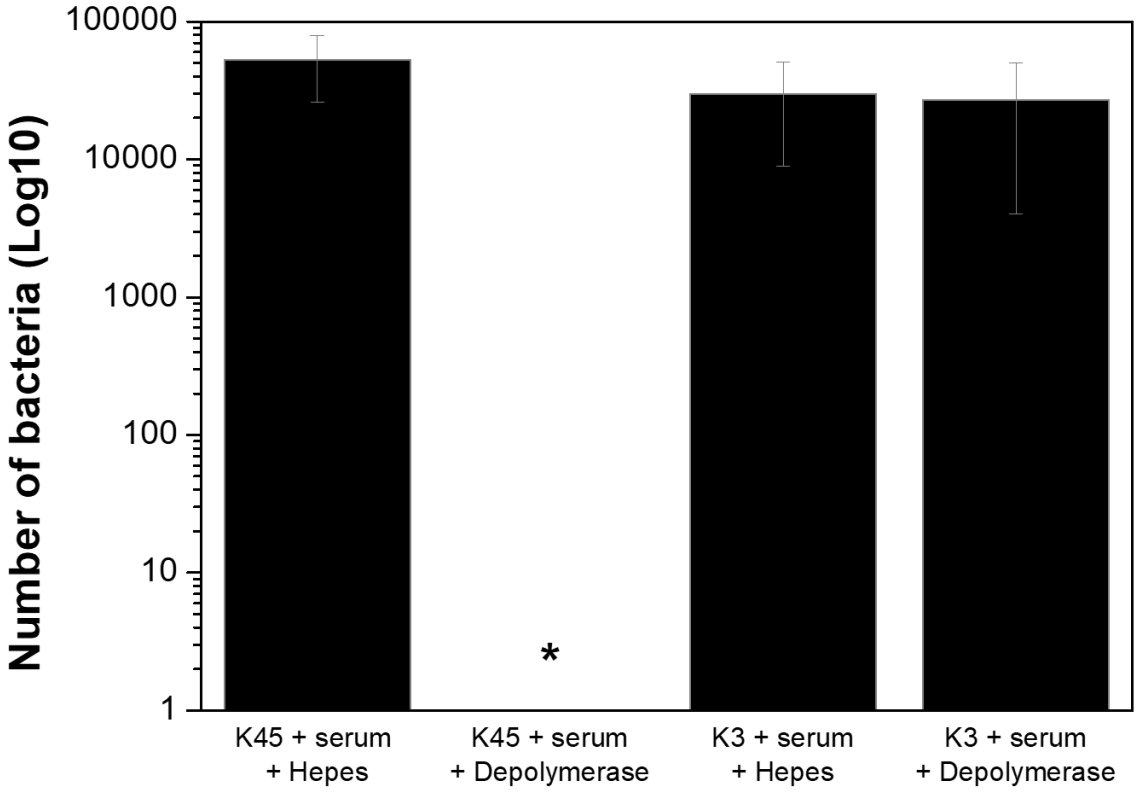

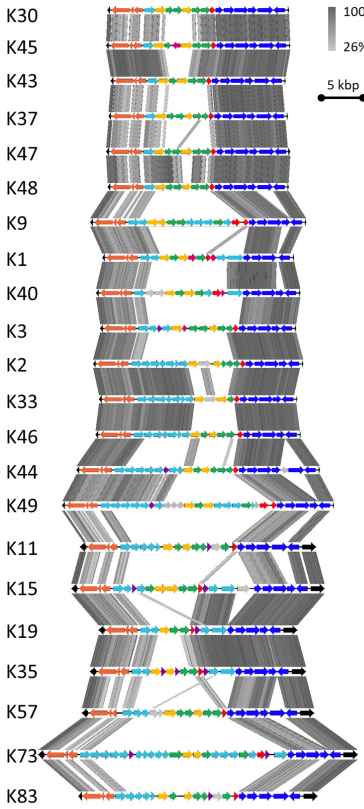


| Species and strain(s) | KL type | fkpA | *wzc/wzb/wza* | *gno* | Variable | | | *wzx* | Variable region | | *wzy* | Variable region | | | *itrB* | *itrA* | Variable | | | *galU* | *ugd* | *gpi* | *gne* | Variable | | | *pgt1* | *pgm* | *lldP* |
|---|---|---|---|---|---|---|---|---|---|---|---|---|---|---|---|---|---|---|---|---|---|---|---|---|---|---|---|---|---|
| *A. baumannii* NIPH 190 | 30 | fkpA | wzc wzb wza | gno | | | | wzx | gtr61 | gtr62 | wzy | gtr63 | gtr50 | | | itrA2 | | | | galU | ugd | gpi | gne1 | | | | pgt1 | pgm | lldP |
| *A. baumannii* NIPH 201 | 45 | fkpA | wzc wzb wza | gno | | | | wzx | gtr89 | gtr13 | wzy | gtr93 | gtr50 | | | itrA3 | | | | galU | ugd | gpi | gne1 | | | | pgt1 | pgm | lldP |
| *A. baumannii* NIPH 60 | 43 | fkpA | wzc wzb wza | gno | | | | wzx | gtr85 | | wzy | gtr49 | gtr50 | | | itrA3 | | | | galU | ugd | gpi | gne1 | | | | pgt1 | pgm | lldP |
| *A. baumannii* NIPH 146 | 37 | fkpA | wzc wzb wza | gno | | | | wzx | gtr75 | grt76 | wzy | gtr77 | gtr99 | | | itrA2 | | | | galU | ugd | gpi | gne1 | | | | pgt1 | pgm | lldP |
| *A. baumannii* NIPH 601 | 47 | fkpA | wzc wzb wza | gno | | | | wzx | gtr95 | gtr96 | wzy | gtr49 | gtr50 | | | itrA3 | | | | galU | ugd | gpi | gne1 | | | | pgt1 | pgm | lldP |
| *A. baumannii* NIPH 615 | 48 | fkpA | wzc wzb wza | gno | | | | wzx | gtr95 | gtr97 | wzy | gtr98 | gtr99 | | | itrA3 | | | | galU | ugd | gpi | gne1 | | | | pgt1 | pgm | lldP |
| *A. baumannii* NIPH 80 | 9 | fkpA | wzc wzb wza | gno | gnaB | | | wzx | | | wzy | gtr21 | gtr22 | FNL | gtr20 | qnr | trB2 | itrA2 | | | galU | ugd | gpi | gne1 | | | | pgm | lldP |
| *A. baumannii* NIPH 290 | 1 | fkpA | wzc wzb wza | gno | gne2 | | | wzx | gtr1 | | wzy | atr1 | gtr2 | | | | | itrA1 | qhbA | qhbB | gdr | galU | ugd | gpi | | | | | pgm | lldP |
| *A. baumannii* ANC 4097 | 40 | fkpA | wzc wzb wza | gno | rmnA | rmnB | | wzx | gtr85 | | wzy | gtr56 | qnr | | | | trB1 | | gtr3 | | gdr | galU | ugd | gpi | gne1 | | | | pgm | lldP |
| *A. baumannii* NIPH 501 | 3 | fkpA | wzc wzb wza | gno | DGA | | | wzx | atr2 | gtr6 | gtr7 | wzy | gtr8 | gtr8 | | | | itrA2 | | | | galU | ugd | gpi | gne1 | | | | pgm | lldP |
| *A. baumannii* NIPH 2061 | 2 | fkpA | wzc wzb wza | gno | PSA | | | wzx | kpsS1 | | | wzy | gtr3 | gtr4 | gtr5 | | | itrA2 | | | | galU | ugd | gpi | gne1 | | | | pgm | lldP |
| *A. baumannii* NIPH 67 | 33 | fkpA | wzc wzb wza | gno | PSA | | | wzx | kpsS2 | | | wzy | gtr5 | | | | | itrA2 | | | | galU | ugd | gpi | gne1 | | | | pgm | lldP |
| *A. baumannii* NIPH 329 | 46 | fkpA | wzc wzb wza | gno | PSA | | | wzx | gtr | | | wzy | gtr14 | gtr15 | | | | itrA2 | | | | galU | ugd | gpi | gne1 | | | | pgm | lldP |
| *A. baumannii* NIPH 70 | 44 | fkpA | wzc wzb wza | gno | LGA1 | | | wzx | gtr56 | | | wzy | gtr57 | gtr58 | gtr5 | | | itrA2 | | | | galU | ugd | gpi | gne1 | Trsp | | | pgt1 | pgm | lldP |
| *A. baumannii* NIPH 335 | 49 | fkpA | wzc wzb wza | gno | LGA | ELA | | wzx | gtr100 | | | wzy | FNL | gtr20 | qnr1 | Unk | | trB2 | itrA3 | | | galU | ugd | gpi | gne1 | | | | | pgm | lldP |
| *A. baumannii* J9 | 11 | fkpA | wzc wzb wza | gno | RML | | | wzx | gtr26 | | | wzy | gtr27 | gtr28 | atr6 | tle | gtr29 | | itrA3 | | | galU | ugd | gpi | | | | | pgt1 | pgm | lldP |
| *A. baumannii* A85 | 15 | fkpA | wzc wzb wza | gno | DGA | gtr34 | | wzx | | | | wzy | gtr35 | gtr36 | | | | | itrA1 | qhbC | qhbB | gdr | Unk | galU | ugd | gpi | gne1 | | | | pgm | lldP |
| *A. baumannii* RBH2 | 19 | fkpA | wzc wzb wza | gno | gne2 | | | wzx | gtr41 | gtr2 | | | | | | | | | itrA1 | qhbC | qhbB | gdr | | galU | ugd | gpi | gne1 | | | | pgm | lldP |
| *A. baumannii* LUH5535 | 35 | fkpA | wzc wzb wza | gno | gne2 | | | wzx | gtr16 | | | wzy | gtr17 | gtr71 | gtr40 | | | | itrA1 | qhbC | qhbB | gdr | | galU | ugd | gpi | gne1 | | | | pgm | lldP |
| *A. baumannii* BAL_212 | 57 | fkpA | wzc wzb wza | gno | RML1 | | | wzx | gtr115 | gtr116 | | wzy | gtr117 | gtr59 | | | | | itrA1 | | | | | galU | ugd | gpi | gne1 | | | | pgt1 | pgm | lldP |
| *A. baumannii* SGH0703 | 73 | fkpA | wzc wzb wza | gno | LGA | ACI | gtr59 | wzx | | | | wzy | gtr30 | FNL | gtr31 | fnr1 | | trB3 | | atrZ | gdr | | galU | ugd | gpi | gne1 | | | | | pgm | lldP |
| *A. baumannii* LUH5538 | 83 | fkpA | wzc wzb wza | gno | RML | | | wzx | gtr154 | | | wzy | gtr27 | gtr60 | atr8 | tle | gtr29 | | itrA3 | | | galU | ugd | gpi | | | | | pgt1 | pgm | lldP |

Capsule export
Nucleotide-sugar biosysthesis
Acetyl or Acyl transferase (atr)
Repeat unit processing
Glycosyltransferase (gtr)
Initiating transferase (itr)
Pathway intermediate and biosynthesis of Glucose derivatives
Other or unkown

PSA: psaA psaB psaC psaD psaE psaF
ELA: elaA elaB elaC
RML: rmlB rmlD rmlA rmlC
RML1: rmlB rmlA fdtA fdtB
ACI: aciA aciE aciC aciD

LGA: lgaA lgaB lgaC lgaD lgaE lgaF
LGA1: lgaA lgaB lgaC lgaH lgaI lgaF lgaG
FNL: fnlA fnlB fnlC
DGA: dgaA dgaB dgaC

**Table 1. *Acinetobacter baumannii* strains used in this study.** For all strains, the specimen, origin, sequence types (ST) according the multilocus sequence analysis, capsular type (K) and respective accession numbers are given. Sequence types refer to the Pasteur scheme. Allocation of the capsular genes and respective coordinates are provided in the GenBank accession no. column. K-type - determined capsule structure; N/A - capsule structure is not available.

| Strain classification and designation | Specimen | Locality and year of isolation | ST | K type | GenBank accession No. | Reference |
|---|---|---|---|---|---|---|
| ***Acinetobacter baumannii*** (n=28) | | | | | | |
| NIPH 501$^{T}$ (= ATCC 19606$^{T}$) | Urine | Before 1949 | ST52 | 3 | KB849970.1 (174731-119233 bp) | (23) |
| NIPH 60 (= CIP 110424) | Sputum | Praha, Czech Republic, 1992 | ST34 | 43 | KB849508.1 (140959-120981 bp) | (23) |
| NIPH 67 (= CIP 110425) | Tracheal secretion | Praha, Czech Republic, 1992 | ST35 | 33 | KB849903.1 (1301423-1278652 bp) | (23) |
| NIPH 70 (= CIP 110426) | Tracheal secretion | Praha, Czech Republic, 1992 | ST36 | 44 | KB849923.1 (574942-546765 bp) | (23) |
| NIPH 80 (= CIP 110427) | I. V. cannula | Praha, Czech Republic, 1993 | ST37 | 9 | KB849944.1 (156383-131489 bp) | (23) |
| NIPH 146 (= CIP 110428) | Wound | Praha, Czech Republic, 1993 | ST25 | 37 | KB849308.1 (572444-592959 bp) | (23) |
| NIPH 190 (= CIP 110429) | Tracheal secretion | Praha, Czech Republic, 1993 | ST9 | 30 | KB849477.1 (592918-572137 bp) | (23) |
| NIPH 201 (= CIP 110430) | Nasal swab | Liberec, Czech Republic, 1992 | ST38 | 45 | KB849844.1 (365379-344305 bp) | (23) |
| NIPH 329 (= CIP 110432) | Tracheal secretion | Tábor, Czech Republic, 1994 | ST11 | 46 | KB849871.1 (2591085-2567472 bp) | (23) |
| NIPH 335 (= CIP 110433) | Sputum | Tábor, Czech Republic, 1994 | ST10 | 49 | KB849886.1 (1318556-1286966 bp) | (23) |
| NIPH 528 (= CIP 110436 = RUH 134) | Urine | Rotterdam, the Netherlands, 1982 | ST2 | 9 | KB849906.1 (78004-102899 bp) | (23) |
| NIPH 601 (= CIP 110437) | Urine | Praha, Czech Republic, 1993 | ST40 | 47 | KB849894.1 (3226845-3205785) | (23) |
| NIPH 615 (= CIP 110438) | Tracheal secretion | Praha, Czech Republic, 1994 | ST12 | 48 | KB849301.1 (114143-93442 bp) | (23) |
| NIPH 1734 (= CIP 110466) | Sputum | Mladá Boleslav, Czech Republic, 2001 | ST15 | 49 | KB849325.1 (2998512-2965610 bp) | (23) |
| NIPH 2390 (= RUH 2180) | Sputum | Nijmegen, the Netherlands, 1987 | ST27 | N/A | N/A | (23) |
| NIPH 2778 (= LUH 8088) | Sputum | Leiden, the Netherlands, 2002 | ST48 | N/A | N/A | (23) |
| NIPH 2783 (= LUH 8326) | Wound | Leiden, the Netherlands, 2002 | ST18 | N/A | N/A | (23) |
| NIPH 290 (= CIP 110431) | Urine | Příbram, Czech Republic, 1994 | ST1 | 1 | KB849940.1 (126651-104645 bp) | (24) |
| NIPH 2061 (= CIP 110467) | I. V. cannula | Příbram, Czech Republic, 2003 | ST2 | 2 | KB849309.1 (77375-101575 bp) | (24) |
| ANC 4097 (= CIP 110499) | Tracheal aspirate | Ústí nad Labem, Czech Republic, 2011 | ST1 | 40 | KB849962.1 (39134-62621 bp) | (24) |
| ANC 4373 | Wound swab | Praha, Czech Republic, 2012 | N/A | N/A | N/A | (23) |
| J9 | N/A | Sydney, Australia, 1999 | ST49 | 11 | KF002790 | (26) |
| A85 | sputum | Sydney, Australia, 2003 | ST1 | 15 | KC118540 (8456-36738 bp) | (27) |
| RBH2 | Other | Brisbane, Australia, 1999 | ST111 | 19 | KU165787 | (28) |
| LUH5535 | N/A | N/A | N/A | 35 | KC526896 | (29) |
| BAL_212 | N/A | Vietnam | ST52 | 57 | KY434631 | (30) |
| SGH0703 | N/A | Singapore, 2007 | ST2 | 73 | MF362178 | (31) |
| LUH5538 | N/A | Germany | N/A | 83 | KC526898 | (9) |

**Table 2. Activity spectrum on *A. baumannii* capsular types.** Drop test of phage and recombinant depolymerase were spotted in bacterial lawns to visualise activity. For the phage, the relative efficiency of plating (EOP) was calculated as the titer of the phage (PFU/ml) for each isolate divided by the titer for the propagating host and recorded as high (≥ 0.5) or low (< 0.5). EOP was also performed to distinguish productive infection (lysis) from lysis from without phenomena by the appearance of cell lysis only in the first dilution(s) for the latter case. K-type - determined capsule structure; N/A - capsule structure is not available; LFW – lysis from without

| | | B9 phage | | B9gp46 depolymerase |
|---|---|---|---|---|
| **Strain** | **K type** | **Infectivity** | **EOP** | |
| NIPH 501$^{T}$ | 3 | - | - | - |
| NIPH 60 | 43 | - | - | - |
| NIPH 67 | 33 | - | - | - |
| NIPH 70 | 44 | - | - | - |
| NIPH 80 | 9 | - | - | - |
| NIPH 146 | 37 | - | - | - |
| NIPH 190 | 30 | - | LFW | + |
| NIPH 201 | 45 | + | High | + |
| NIPH 329 | 46 | - | - | - |
| NIPH 335 | 49 | - | - | - |
| NIPH 528 | 9 | - | - | - |
| NIPH 601 | 47 | - | - | - |
| NIPH 615 | 48 | - | - | - |
| NIPH 1734 | 49 | - | - | - |
| NIPH 2390 | N/A | - | - | - |
| NIPH 2778 | N/A | - | - | - |
| NIPH 2783 | N/A | - | - | - |
| NIPH 290 | 1 | - | - | - |
| NIPH 2061 | 2 | - | - | - |
| ANC 4097 | 40 | - | - | - |
| NIPH 4373 | N/A | - | - | - |
| J9 | 11 | - | - | - |
| LUH5554 | 15 | - | - | - |
| A85 | 15 | - | - | - |
| RBH2 | 19 | - | - | - |
| LUH5535 | 35 | - | - | - |
| BAL_212 | 57 | - | - | - |
| SGH0703 | 73 | - | - | - |

**Table 3. Activity spectrum of depolymerase B9gp69 on *A. baumannii* isolated in this study.** K45 NIPH 201 cells were incubated with SM buffer, phage or B9gp69 and afterwards tested for their sensitivity against the phage or the B9gp69 using drop tests. For the phage, the relative efficiency of plating (EOP) was calculated as the titer of the phage (PFU/ml) for each isolate divided by the titer for the propagating host and recorded as high (≥ 0.5) or low (< 0.5). EOP was also performed to distinguish productive infection (lysis) from lysis from without phenomena by the appearance of cell lysis only in the first dilution(s) for the latter case.

| Strains | incubated with SM buffer | | incubated with phage | | incubated with depolymerase | |
|---|---|---|---|---|---|---|
| Isolate n. | Phage (EOP) | Depolymerase | Phage (EOP) | Depolymerase | Phage (EOP) | Depolymerase |
| Isolate #1 | + (high) | + | + (high) | + | + (high) | + |
| Isolate #2 | + (high) | + | + (high) | + | + (high) | + |
| Isolate #3 | + (high) | + | - | - | + (high) | + |
| Isolate #4 | + (high) | + | - | - | + (high) | + |
| Isolate #5 | + (high) | + | + (low) | + | + (high) | + |
| Isolate #6 | + (high) | + | + (high) | + | + (high) | + |
| Isolate #7 | + (high) | + | + (low) | + | + (high) | + |
| Isolate #8 | + (high) | + | + (low) | + | + (high) | + |
| Isolate #9 | + (high) | + | + (high) | + | + (high) | + |
| Isolate #10 | + (high) | + | - | - | + (high) | + |